

ASSESSMENT OF AN ADVANCED PEDESTRIAN DUMMY
FOR USE IN FULL-SCALE CASE RECONSTRUCTIONS

NHTSA TECHNICAL REPORT
DOT HS 809 391

Jason Stammen
Brian Ko

Vehicle Research & Test Center
National Highway Traffic Safety Administration
July 9, 2001

Executive Summary

Honda R&D has recently designed an advanced pedestrian dummy (Polar II). This dummy is similar in size and stature to the Hybrid III 50th percentile male, and it has recent biomechanical data incorporated into the design of its components. This prototype dummy was made available to the NHTSA Vehicle Research & Test Center (VRTC) for developmental testing with the HYGE Impact Simulator (Transportation Research Center, Inc.). Two PCDS (Pedestrian Crash Data Study) cases, involving a low (1999 Honda Civic) and high (1991 Chevrolet Silverado) front-end profile, were selected from this database for reconstruction using the Polar II dummy.

The objectives of this project were as follows:

1. Develop a full-scale pedestrian sled test procedure that can incorporate different vehicle models and replicate vehicle damage patterns observed in cases
2. Evaluate the trajectories of head, knee, pelvis, and foot and compare with biofidelic performance corridors and computer simulation results for impact with a similar vehicle profile
3. Compare dummy measurements with injuries observed in cases and compare with human injury tolerances
4. Evaluate durability of the dummy

A pedestrian sled buck was designed and fabricated, and the first series of tests involved impact of the dummy with a 1999 Honda Civic. The speed of the vehicle was approximately 48 km/hr (30 mph) at the time of impact, and the vehicle was rotated to 17 degrees relative to the path of the vehicle. Five tests were allowed for replication of vehicle damage patterns with the actual case. In the Silverado test series, the dummy was impacted on its left side by the front right side of the vehicle. Uncertainties about the ability of the dummy to withstand a high velocity, high profile impact prevented exact replication of a PCDS case with the Silverado; the kinematics of the dummy in response to a high profile impact and the effect of velocity change on head/neck motion were the main objectives. Three tests were done at 20 km/hr (12.4 mph), and two were done at 25 km/hr (15.5 mph).

After analysis of dummy measurements and trajectories, it was determined that the third Civic test came closest to replication of the actual case. The HIC was consistent with the head injuries suffered by the pedestrian, and the damage patterns on the vehicle were similar to the measured contact points from the case. It was also determined that elevation of the dummy was directly related to WAD (wrap around distance) and curvature of the head trajectory. Pedestrian orientation relative to the vehicle was also found to affect head and pelvis motion. The head traveled higher and farther when the dummy was rotated away (facing down the track) from the vehicle. The pelvis trajectory of a dummy facing perpendicular to the track increases in height, but the pelvis moves in the opposite direction when the dummy is rotated away from the vehicle. From these results, it was reasonable to estimate that the pedestrian in the case was facing away from the vehicle at impact and was elevated off the ground some distance, either as a result of jogging (which was reported) or jumping.

Measurements in the Silverado cases were estimated for the speed of 50 km/hr (velocity in the actual case), and there was some agreement, but nothing conclusive. Velocity did have an effect on the horizontal displacement of the head in these tests, with the 25-km/hr tests resulting in higher translations (roughly 9 cm) than 20 km/hr tests. The arm and leg positions were varied for these tests, causing more changes in kinematics. Moving the right leg in front of the left as if the dummy were walking resulted in a higher trajectory of the head and subsequent increase of 4 cm in horizontal translation. The position of the hands and arms also changed the kinematics. Tying the hands together in front of the dummy resulted in a lower translation (5 cm) than when the arms were bent at 90 degrees at the sides, most likely because the arms were closer to the body and therefore the head did not have as far to travel for impact with the hood.

Overall, the damage to the dummy was minimal considering the violent nature of the tests. The legs held up well. The left tibia was replaced prior to each Civic test and was not damaged during the entire series. The major problems occurred in the neck, and changes to the assembly or materials are recommended. In terms of reconstructing cases with the Polar dummy, it seems that we can get close to what happened in the accident, but it is currently very difficult to match a case exactly by using the dummy.

Table of Contents

1.	Introduction.....	4
2.	Methods.....	5
2.1.	Pedestrian Sled Buck Design and Fabrication.....	5
2.1.1	Buck Frame.....	5
2.1.2	Vehicle Attachment/Preparation.....	6
2.2	Dummy Standing System.....	7
2.3	Dummy Preparation.....	7
2.4	Test Procedure.....	7
2.4.1	General Test Setup.....	7
2.4.2	Cameras.....	8
2.4.3	Dummy Stance.....	8
2.4.4	Release Timing.....	9
2.4.5	Targets and Dummy Paint.....	9
2.4.6	Vehicle Damage Locations.....	9
2.4.7	Data Acquisition.....	10
3.	Civic Results.....	10
3.1	Test 1.....	10
3.2	Test 2.....	12
3.3	Test 3.....	14
3.4	Test 4.....	15
3.5	Test 5.....	17
4.	Silverado Results.....	19
4.1	Test 1.....	19
4.2	Test 2.....	21
4.3	Test 3.....	22
4.4	Test 4.....	24
4.5	Test 5.....	25
5.	Discussion.....	27
5.1	Civic Tests.....	27
5.2	Silverado Tests.....	30
5.3	Durability.....	33
5.4	Sled Buck.....	35
6.	Conclusions/Recommendations.....	35
7.	References.....	36
8.	Appendix.....	38
8.1	Summary Table of Peak Data.....	38
8.2	Summary Table of Calculations.....	38
8.3	Injury Tolerances.....	39
8.4	Accident Case Injuries and Transducers used for Comparison.....	39
8.5	Dummy Stance Dimensions.....	40
8.6	Transducer List.....	41
8.7	Channels for Each Test.....	42
8.8	Data Plots.....	

1. Introduction

Full-scale experimental testing that investigates collisions between pedestrians and vehicles is not a new concept. Several studies have been done using either dummies or post-mortem human subjects (PMHS) to evaluate the kinematics and impact measurements associated with pedestrian response to vehicle impact. In the mid 1970's, pedestrian fatalities in the U.S. numbered 7,000 to 8,000 per year. It became apparent through research that the shape and structural integrity of a vehicle's front end had a direct effect on injury severity and occurrence. In response, automobile manufacturers incorporated more streamlined, less aggressive front ends into their new vehicle models over the years. In the present day, pedestrian fatalities in the U.S. have steadily declined to below 5,000 per year. It can be argued that this decrease can be attributed to a decrease in alcohol-related accidents or other traffic safety programs such as improved traffic intersections and education of young people. While these factors certainly have an effect, it is believed that improving current vehicle designs through continuing pedestrian research can reduce these statistics further.

A study by Schneider, et al (1974) looked at the effect of vehicle speed on damage patterns for different profiles when comparing accident cases with experimental results [1]. They concluded that contact of a pedestrian with a windshield must be expected at impacts considerably below the pedestrian's c.g. above 40 km/hr (25 mph). In the cases of impacts closer to the pedestrian c.g., windshield contact should be expected at vehicle speeds at or above 60 km/hr (37 mph). The major conclusion, however, was that experimental results may be applied to analysis and reconstruction of actual accident cases. Pritz, et al (1975) discovered that injuries to the lower body of adult pedestrians are strongly dependent upon vehicle design, as well as an injury tolerance threshold for pelvic acceleration [2]. Stcherbatcheff, et al (1975) reported that the severity of impacts of various parts of the body, in particular the head, is linked to the profile of the vehicle involved [3]. Bacon, et al (1976) analyzed the effects of bumper height, lead, and deflection characteristics on leg impact measurements. They reported positional requirements of the bumper for decreased leg injury severity but state that the vehicle front-end height is more important in decreasing injury severity of critical body parts such as the head [4]. Krieger, et al (1976) compared the responses of cadavers and 95th percentile dummies for identical collision conditions and noted that they were quite different [5]. In another study comparing dummies with human anatomic specimens, Pritz, et al (1978) impacted one of each simultaneously with an identical vehicle cantilevered off each side of the basic HYGE impact sled simulator. It was determined that the dynamic performance of the Part 572 adult dummy, modified for this application, was similar to that of the cadaveric specimen, especially in the lower body response [6]. Finally, Ravani, et al (1981) identified five basic kinematic trajectories for frontal collision cases and analyzed each type's relative injury risks [7]. From this summary of relevant studies, two distinct issues stand out. First, vehicle front-end modifications have an effect on pedestrian injury reduction. Second, there is no available pedestrian dummy incorporating recent biomechanical data.

Honda R&D has recently designed an advanced pedestrian dummy (Polar II) that is being manufactured by GESAC (Boonboro, MD) [8]. This dummy is similar in size and stature to the Hybrid III 50th percentile male, and it has recent biomechanical data incorporated into the design of its components. It is a modified Thor model, with revisions to the neck, shoulder, lumbar joint, and leg for lateral response. In particular, the leg is completely revamped, with a biofidelic knee joint and flexible tibia. The tibia was designed to be more flexible after Honda determined that lower leg rigidity has a direct influence on head velocity at impact. The shoulder was made to be more flexible than earlier versions after it was determined that rigidity increases "bouncing" of the dummy, which is not similar to PMHS response. The neck is also very different, with front and rear tension cables to simulate muscle tension. Finally, the lumbar joint was also made less rigid to allow the pelvis motion to fall into biomechanical trajectory corridors. This prototype dummy was made available to the NHTSA Vehicle Research & Test Center (VRTC) for developmental testing with the HYGE Impact Simulator (Transportation Research Center, Inc.).

The Pedestrian Crash Data Study (PCDS) was conducted by NHTSA from July 1994 to December 1998 [9]. During that time, detailed crash reconstruction data was conducted at six sites across the United States on 521 pedestrian-vehicle collisions. Two cases, involving a low (1999 Honda Civic) and high (1991 Chevrolet Silverado) front-end profile, were selected from this database for reconstruction using the Polar II dummy. The selection was based on the height and weight of pedestrian, acceptable vehicle impact

speed, completeness of case information, and availability of a matching vehicle model. The Civic case involved a 34-yr old male (height 178 cm, weight 75 kg) colliding with a vehicle traveling at 46-48 km/hr. The pedestrian's head impacted the passenger side of the windshield, and he sustained AIS 1-2 injuries to the head, arms, and legs.

Uncertainties about the ability of the dummy to withstand a high velocity, high profile impact prevented exact replication of a PCDS case with the Silverado; the kinematics of the dummy in response to a high profile impact and the effect of velocity change on head/neck motion were the main objectives. The case that was selected as a baseline reference involved a severe collision with a 77-yr old female (height 169 cm, weight 70 kg), in which the pedestrian sustained five broken ribs and punctured lung (AIS 4) and multiple AIS 1-3 injuries to the legs and head as well.

The objectives of this project were as follows:

5. Develop a full-scale pedestrian sled test procedure that can incorporate different vehicle models and replicate vehicle damage patterns observed in cases
6. Evaluate the trajectories of head, knee, pelvis, and foot and compare with biomechanical corridors and computer simulation results
7. Compare dummy measurements with injuries observed in cases and compare with human injury tolerances
8. Evaluate durability of the dummy
9. Summarize information useful for IHRA test procedure development

2. Methods

2.1. Pedestrian Sled Buck Design and Fabrication

2.1.1. Buck Frame

In order to perform full-scale sled tests, a pedestrian sled buck was designed and fabricated. Several configurations were suggested, but only one design fully incorporated a majority of the conditions present in the case. This design has the buck extending seven feet laterally from each side of the sled (total of 19' in width), with the test vehicle balanced by the appropriate ballast weight on the opposite side (Figure 2.1). Diagonal braces that attach the two ends of the buck to the sled prevented rotation of the buck. The frame was constructed from 4" x 6" x 3/16" steel rectangular tubing, and the sled attachment plates (1/2" cold-drawn steel) were welded directly to it. Thirty thru holes (3/4" diameter) were located on the ten plates to facilitate 5/8" diameter bolts for sled attachment.

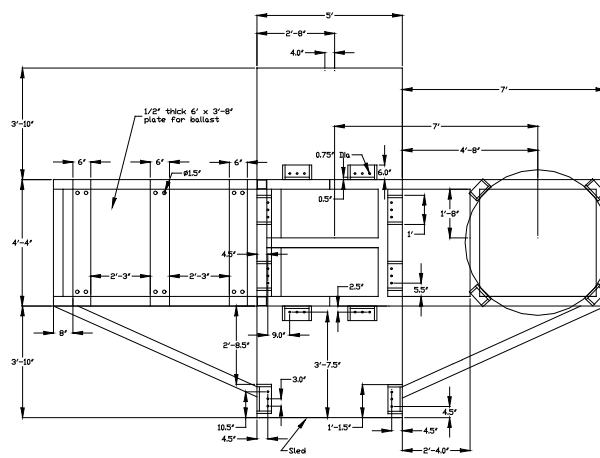


Figure 2.1. Top view of buck as it attaches to the HYGE sled

2.1.2. Vehicle Attachment/Preparation

Since pedestrian accidents involve a wide range of vehicles, the buck was designed accordingly. A circular ½” thick, 5’ diameter steel plate was used as the interface between the buck and vehicle. This shape was chosen to allow vehicle rotation, as is occasionally necessary when attempting to reconstruct an accident. Holes could be drilled to match the bottom frame of most vehicles, and the disc could then be rotated to the specified angle and bolted in place (Figure 2.2). For this study, the bottom frames of the Civic and Silverado were fabricated so that the center of gravity of the vehicle was near the center of the disc to prevent any unbalance in the vertical direction (Figure 2.3).

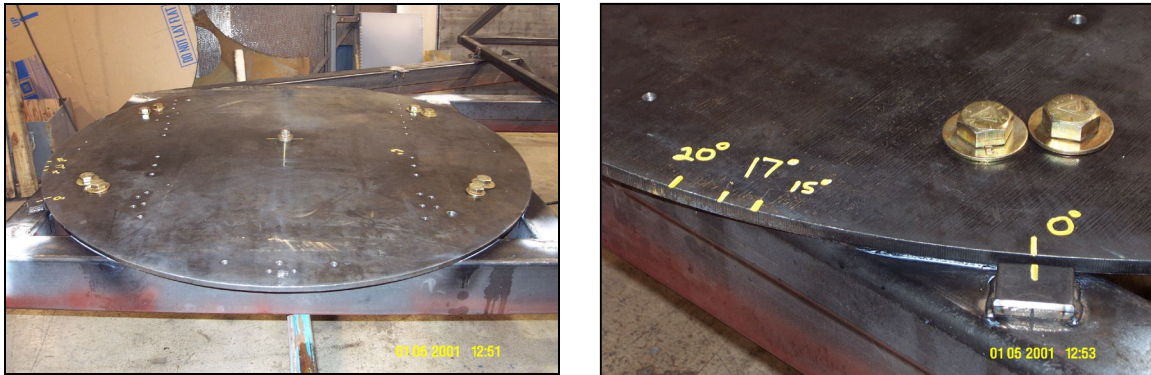


Figure 2.2. Vehicle interface plate with rotation capability



Figure 2.3. Civic (left) and Silverado (right) with frame for buck attachment

Half-inch diameter bolts were used to attach the vehicles to the disc, and the minimum number bolts were calculated to be 15 for the Silverado and 10 for the Civic, based on a 10 g sled acceleration pulse. With a factor of safety incorporated into the design, 26 bolts were used for the Silverado and 14 bolts were used for the Civic (Table 2.1).

Attachment	Bolt Size (in)	Static Weight (lbs)	Bolt Torque (ft-lbs)	Dynamic Force @ 10 g (lbs)	Minimum Required Bolts	Actual Bolt Number	Safety Factor
Buck to Sled ¹	0.625	7,160	19	71,600	28	30	1.1
Civic to Interface Disc	0.500	1,700	21	17,000	10	14	1.4
Silverado to Interface Disc	0.500	2,800	22	28,000	15	26	1.7
Interface Disc to Buck ¹	1.000	3,300	82	33,000	5	8	1.6

Table 2.1. Bolt calculations

¹ For Silverado case

To decrease the weight of the vehicles, they were cut behind the B-pillars and the interior was stripped. In addition, the doors were taken off. The bottom frames were fabricated from 2"x 2" square tubing (1/8" wall thickness).

2.2. Dummy Standing System

The Polar dummy was unable to stand without support. A magnetic release mechanism was built to allow electrically controlled release of the dummy prior to impact by the vehicle. An electromagnet was purchased (Storch Magnetics, Inc.) based on its static holding capacity. This capacity had to be greater than the weight of the dummy (70 kg). A latch mechanism was fabricated based on the design parameters of the magnet (Figure 2.4). Deactivation of the magnet triggers the release of the dummy via a rotating member, which is pulled downward almost instantaneously by the weight of the standing dummy.

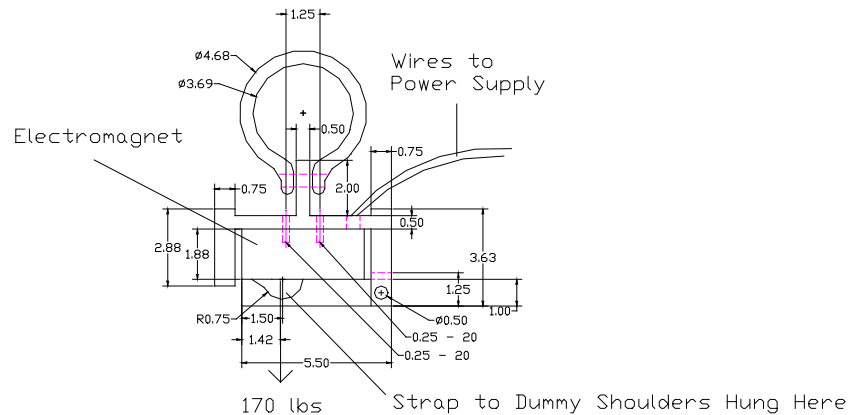


Figure 2.4. Magnetic release mechanism in the closed (pre-impact) position

2.3. Dummy Preparation

The Polar II dummy came fully assembled for conventional data acquisition. The only preparation issues involved adaptation of the sensors to the TRC data acquisition system and sensor function checks. The dummy was instrumented with three triaxial accelerometers (head, thorax, pelvis), two uniaxial accelerometers (femur, tibia), and seven load cells (neck, femur, tibia) for a total of 12 transducers. These transducers yielded 32 channels of information (see Appendix 8.7). Relay cables (50 cm in length) for conversion from the 6-pin (Omnetics, Inc.) to standard 9-pin connectors were assembled for all 32 channels. After connection of the umbilical to the sensors, impedance checks were done to verify proper electrical conductivity. Polarity checks were done prior to the first test (J211 sign convention), and the sensors were checked prior to each test.

2.4. Test Procedure

2.4.1. General Test Setup

The first series of tests involved impact of the dummy with a 1999 Honda Civic. Since the dummy was instrumented only on the left side, the test was set up to be a symmetrical representation of the actual case, where the pedestrian was impacted on the right side (Figure 2.5). The path of the pedestrian from bumper impact point to windshield impact point was calculated to be 17 degrees based on the longitudinal and lateral measurements made on the vehicle during post-accident inspection. The sled buck was designed to allow vehicle rotation between 15 and 20 degrees (2-3 degrees clockwise and counterclockwise from the calculated pedestrian travel angle of 17 degrees) in case modifications had to be made between tests. Because of this angle and projected travel of the dummy into the sled, a protective net was attached to the buck. The speed of the vehicle was approximately 48 km/hr (30 mph) at the time of impact. It was

expected that at most one test would be done per day due to the time needed for 24-hour windshield curing, vehicle part replacement, dummy repair, and vehicle rotation. Five tests were allowed for replication of vehicle damage patterns with the actual case.



Figure 2.5. Civic Test Setup

A 1999 Chevrolet Silverado was used for the high profile vehicle test series. In this set, the dummy was impacted on its left side by the front right side of the vehicle (Figure 2.6). As mentioned previously, exact replication of the PCDS case was not the main objective of this series; instead, the kinematics of the dummy in response to a high profile impact and the effect of velocity change on head/neck motion were the main objectives. Three tests were done at 20 km/hr (12.4 mph), and two were done at 25 km/hr (15.5 mph). The low speeds were applied because these were the first tests performed with a high profile vehicle, and the durability of the dummy was uncertain. The case that these tests were modeled after involved a vehicle impact speed of around 50 km/hr. Computer simulations done by Honda predicted moderate to heavy dummy damage at 30 km/hr, so care was taken to stay below this velocity.



Figure 2.6. Silverado Test Setup

2.4.2. Cameras

Five cameras were used to record the impact and subsequent trajectory of the dummy. Three high-speed digital cameras and two conventional film cameras were used. Digital cameras were set up behind the dummy so that the targets were in view, with one being dedicated to the entire dummy and post-impact flight. Two other digital high-speed cameras focused on the leg impact from the waist to feet and head impact with the front vehicle surface. A normal high-speed film camera was fixed directly above the dummy (17 ft) to pick up the path of the dummy across the front of the vehicle starting at impact. A final camera was situated perpendicular to the track behind the dummy and served as a backup to the digital camera that picked up the overall dummy kinematics.

2.4.3. Dummy Stance

The initial configuration of the dummy was recorded to find how the stance affected resultant kinematics. Measurements of dimensions such as knee height, heel-to-heel width, and leg bend angles were documented for each test (see Appendix 8.5).

2.4.4. Release Timing

Pulse trials were done to set the velocity of the sled, and the time between launch and attainment of this velocity was recorded. Using video imaging, the time from voltage shutoff to release of the magnetic latch was determined. This time was subtracted from the velocity attainment time to determine how long after launch to deactivate the release magnet:

$$\text{Deactivation Time after Launch} = \text{Velocity Attainment Time} - \text{Latch Release Lag Time}$$

For example, if the sled got to 30 mph in 190 milliseconds after launch, and it took 90 milliseconds for the latch to release after voltage shutoff, the magnet deactivation would be set to occur prior to 100 ms after launch for the dummy to be released right at impact (Figure 2.7). The length of a breakaway switch similar to the sled backup actuation switch could vary this shutoff time. The dummy was found to remain standing for roughly a half second after release, so it was better to deactivate the magnet prior to impact, near the initial launch time.

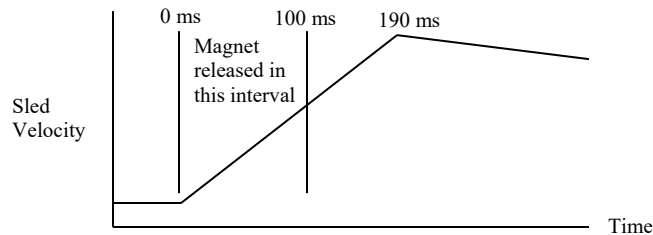


Figure 2.7. Example of the release timing

2.4.5. Targets and Dummy Paint

Four-inch camera targets were placed on important body landmarks to allow image analysis of trajectories (Image Express, version 4.3, SAI), and chalk paint was applied to the left side of the dummy to distinguish between different body regions that contact the vehicle front (Figure 2.8).



Figure 2.8. Target Locations

2.4.6. Vehicle Damage Locations

After installation of a new windshield, hood, and bumper for each test, vehicle/pedestrian contact points were marked off based on case information. Points were sequenced from the initial bumper impact point to the final scuff or dent caused by the pedestrian (Figure 2.9).



Figure 2.9. Contact point designation

2.4.7. Data acquisition

Thirty-two channels of data were acquired for each test and peak values were compared with injury tolerance levels for different body components. The relative displacements of targets were obtained from image analysis of the high-speed video, and specified body trajectories (head, pelvis, knee, and foot for Civic tests) were compared with human biomechanical corridors created from cadaver tests performed with a similar vehicle profile. For the Silverado case, trajectories were also done but not compared with corridors. The main objective was to see the relative displacement of the head to the neck and the influence of velocity on WAD (wrap around distance). Both the dummy and vehicle were inspected after the test. The dummy was inspected for broken components and damaged wiring or transducers. The vehicle was inspected to see how close the dummy path came to the path specified by the sequential case contact points laid out prior to the test. Measurements of damage patterns were used to create dummy path plots for visual comparison of differences between tests, as well as between each test and the actual accident case.

3. Civic Results

3.1. Test 1 (Civic)

The first test consisted of a vehicle angle of 17 degrees, and a pedestrian stance with legs in the same plane and arms bent at the elbow.

3.1.1. Component Trajectories

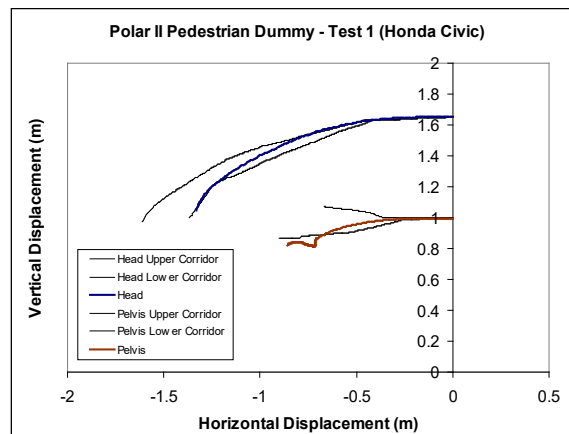


Figure 3.1. Dummy trajectories (target motion analysis) versus PHMS corridors for similar vehicle profile

3.1.2. Overhead Path of Entire Dummy Across Vehicle Front

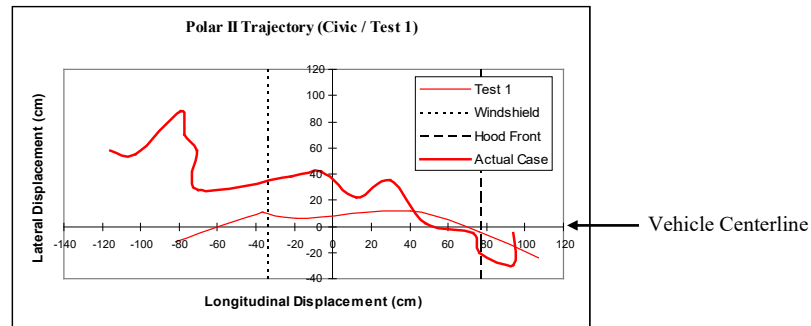


Figure 3.2. Damage patterns and comparison with marked contact points documented from actual case

3.1.3. Head

The head impacted the rigid structure between the bottom of the windshield and top of hood (windshield frame), which was well below the target contact point on the upper right corner of the windshield. The wrap-around distance (WAD) was 182 cm, which was 66 cm less than in the case (248 cm). This caused a high head resultant acceleration of 373.6 g and calculated HIC_{36 ms} value of 3088.

3.1.4. Neck

The upper neck peak forces were -2365 N (y) and 3939 N (z), and the moment about x was 71.9 N-m. The lower neck forces were -2411 N (y) and 4382 N (z), and the lower neck moment about x was -95.1 N-m. The peak front cable tensile force experienced was 604 N, while the rear cable showed 1175 N. The calculated peak moment about the occipital condyle was 51.9 N-m.

3.1.5. Thorax/Pelvis

The left shoulder rotating shaft assembly was fractured in shear at contact with the hood surface, probably due to fatigue (Figure 3.3). The peak chest and pelvis resultant accelerations were 60.7 g and 55.0 g, respectively.

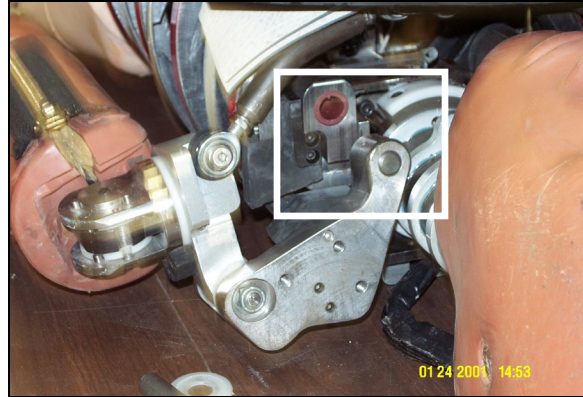


Figure 3.3. Sheared shoulder shaft

3.1.6. Upper Leg

The femur experienced forces of 1216 N (x), -947 N (y), and 5854 N (z). The moment about x was -277.7 N-m, and acceleration in the y direction on the distal medial femur was 287.9 g. The acceleration observed on the lateral side of the femur was 222.7 g. The angular acceleration calculated from these two linear accelerations was 16,474 rad/s² [10].

3.1.7. Lower Leg

The proximal tibia experienced forces of 1659 N (x), 808 N (y), and 5049 N (z). The moment about x was 124.5 N-m. The distal tibia (ankle) forces were -656 N (y) and 3281 N (z), with 105.3 N-m x moment.

3.2. Test 2 (Civic)

For this iteration, the vehicle was rotated 3 degrees to an angle of 20 degrees. This change was based on the path of the dummy in the first test. The dummy was also raised 6.5 inches to increase WAD.

3.2.1. Component Trajectories

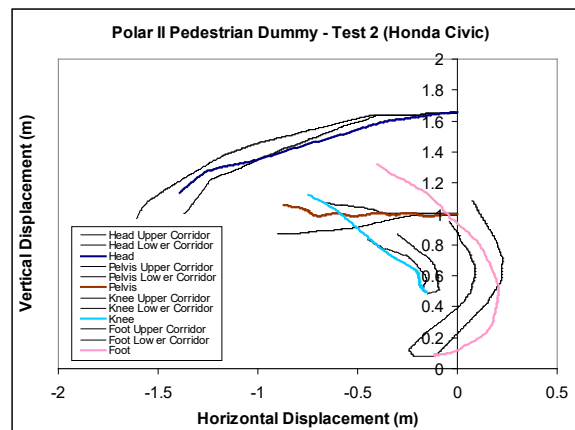


Figure 3.4. Dummy trajectories (target motion analysis) versus PHMS corridors for similar vehicle profile

3.2.2. Overhead Path of Entire Dummy Across Vehicle Front

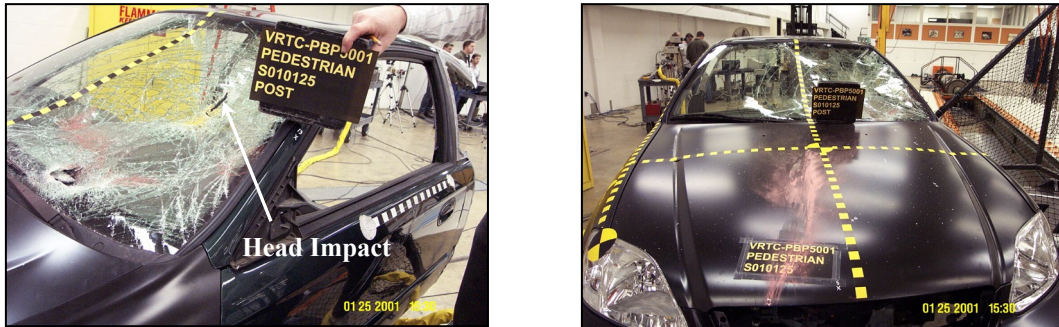
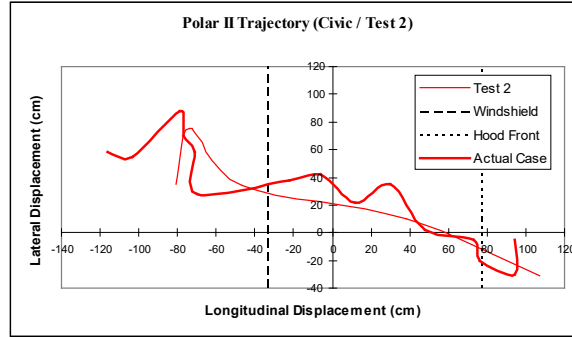


Figure 3.5. Damage patterns and comparison with marked contact points documented from actual case

3.2.3. Head

The head impacted the windshield this time, although still too low (WAD = 222 cm). This caused a much lower head resultant acceleration of 168.7 g and calculated $HIC_{36\text{ ms}}$ value of 1464.

3.2.4. Neck

The upper neck peak forces were -951 N (y) and 3138 N (z), and the peak moment about x was -65.8 N-m. The lower neck forces were 1440 N (y) and 3135 N (z), and the lower neck moment about x was -84.5 N-m. The peak front cable tensile force experienced was 603 N, which was almost identical to Test 1. The rear cable force was much higher, however, with a peak tensile force of 3361 N. This cable failed during the test, and several neck segments were cracked at the interface between rubber and steel, presumably because the loss of the cable support increased the rotation. The calculated peak moment about the occipital condyle was -76.4 N-m.

3.2.5. Thorax/Pelvis

The chest and pelvis resultant accelerations were 66.2 g and 56.5 g, respectively. There was damage similar to the neck in the lumbar flex joint, with small fissures propagating around the circumference of the lowest segment.

3.2.6. Upper Leg

The femur experienced forces of 581 N (x), 546 N (y), and 5224 N (z). The moment about x was -209.8 N-m, and acceleration in the y direction on the distal medial femur was -174.6 g. The acceleration observed on the lateral side of the femur was -236.1 g. The angular acceleration calculated from these two linear accelerations was $-32,338\text{ rad/s}^2$.

3.2.7. Lower Leg

The proximal tibia experienced forces of 2392 N (x), 2264 N (y), and 4782 N (z), which were considerably higher in the x and y directions than Test 1, but slightly lower in the z direction. The moment about x was 126.7 N-m, which was very similar to the Test 1 magnitude. The distal tibia (ankle) had forces of -1329 N (y) and 2069 N (z), with a moment about x of 120.1 N-m.

3.3. Test 3 (Civic)

The angle and elevation of the dummy were unchanged, but the dummy was rotated away from the vehicle.

3.3.1. Component Trajectories

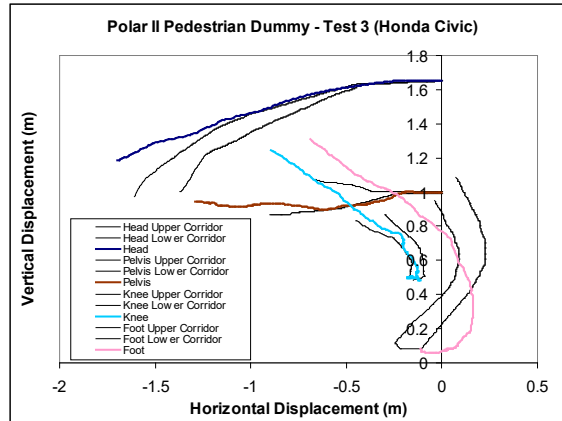


Figure 3.6. Dummy trajectories (target motion analysis) versus PHMS corridors for similar vehicle profile

3.3.2. Overhead Path of Entire Dummy Across Vehicle Front

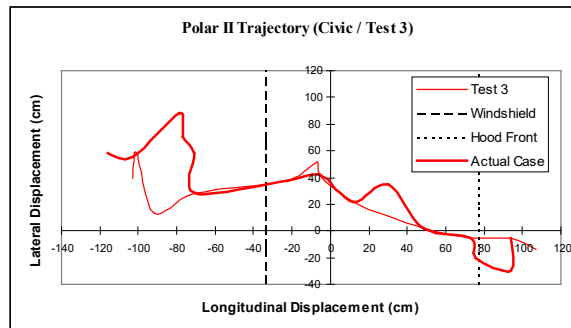


Figure 3.7. Damage patterns and comparison with marked contact points documented from actual case

3.3.3. Head

The head impacted the windshield very close to the case head contact area, although still a little too low (WAD = 239 cm). The head resultant acceleration of 109.9 g and calculated HIC_{36 ms} value of 688 were in the range of an AIS 1-2 head injury [11].

3.3.4. Neck

The upper neck peak forces were -951 N (y) and -2856 N (z), and the peak moment about x was -31.2 N-m. The lower neck forces were 749 N (y) and -3031 N (z), and the lower neck moment about x was -72.4 N-m. The peak front cable tensile force experienced was 226 N, and the rear cable force was 480 N. The calculated peak moment about the occipital condyle was -36.6 N-m. The upper neck x moment, moment about the o.c., and neck y force were all considerably lower than in Test 2.

3.3.5. Chest/Pelvis

The chest and pelvis resultant accelerations were 67.2 g and 115.5 g, respectively. While the chest resultant remained consistent with Test 2, the pelvis acceleration was twice as high. This was most likely due to a fracture of the right hip and subsequent release of the right leg after impact (Figure 3.8). This fracture could have also been from fatigue, or it could have been the direct impact with the vehicle front end. That was not the case in the first two tests, where the legs were in line with one another and the left leg absorbed energy prior to right leg contact.



Figure 3.8. Broken right hip sustained in Test 3

3.3.6. Upper Leg

The femur experienced forces of 555 N (x), -881 N (y), and 3520 N (z). The moment about x was -226.4 N-m, and acceleration in the y direction on the distal medial femur was 138.4 g. The acceleration observed on the lateral side of the femur was 102.5 g. The angular acceleration calculated from these two linear accelerations was 15,643 rad/s².

3.3.7. Lower Leg

The proximal tibia experienced forces of 2982 N (x), 2534 N (y), and 2564 N (z). The moment about x was 188.4 N-m, which was higher than the two previous tests. The distal tibia (ankle) had forces of -1194 N (y) and 2411 N (z), with a moment about x of 115.4 N-m.

3.4. Test 4 (Civic)

Test 3 was by far the closest to the case out of the first three tests. The broken right hip was a deterrent, however, so it was decided that Test 4 would incorporate the same conditions as Test 3 with a replaced right hip joint.

3.4.1. Component Trajectories

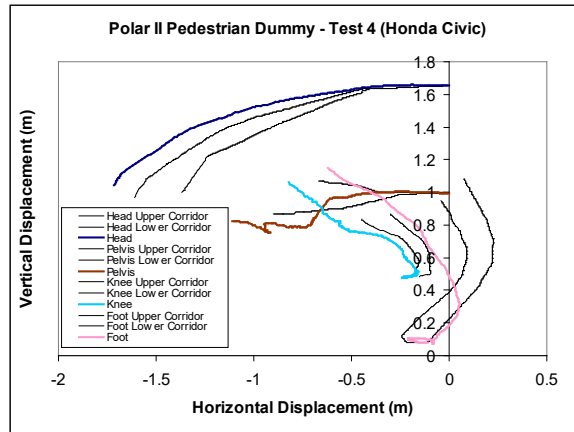


Figure 3.9. Dummy trajectories (target motion analysis) versus PHMS corridors for similar vehicle profile

3.4.2. Overhead Path of Entire Dummy Across Vehicle Front

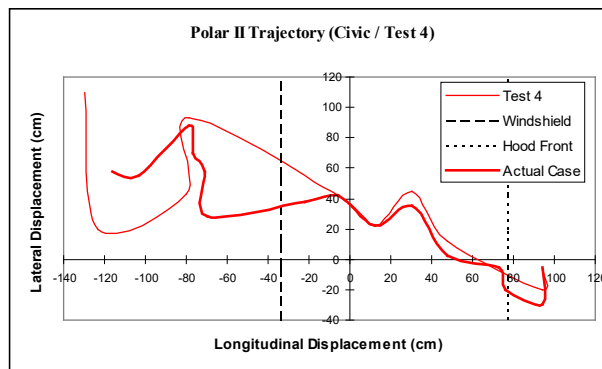


Figure 3.10. Damage patterns and comparison with marked contact points documented from actual case

3.4.3. Head

The head impacted the windshield far short of the case head contact area, near the area hit in Test 2 (WAD = 217 cm). However, this was partially due to the failure of the windshield sealant. It was estimated that the head initially contacted near the case head contact point, but the deformation of the windshield caused

the center of the spider web damage to move closer to the front of the vehicle (Figure 3.11). The head resultant acceleration was 352.5 g, but the calculated HIC_{36 ms} value was 1486.



Figure 3.11. Large displacement of head inside the vehicle because of windshield sealant failure

3.4.4. Neck

The upper neck peak forces were -583 N (y) and 2572 N (z), and the peak moment about x was 40.7 N-m. The lower neck forces were 658 N (y) and 2483 N (z), and the lower neck moment about x was -64.7 N-m. The peak front cable tensile force experienced was 675 N, and the rear cable force was 101 N. The calculated peak moment about the occipital condyle was 41.7 N-m.

3.4.5. Chest/Pelvis

The chest and pelvis resultant accelerations were 42.3 g and 45.2 g, respectively.

3.4.6. Upper Leg

The femur experienced forces of 638 N (x), 733 N (y), and 5045 N (z). The moment about x was -228.3 N-m, and acceleration in the y direction on the distal medial femur was 131.8 g. The acceleration observed on the lateral side of the femur was 108.9 g. The angular acceleration calculated from these two linear accelerations was 11,466 rad/s².

3.4.7. Lower Leg

The proximal tibia experienced forces of 2905 N (x), 2709 N (y), and 3836 N (z). The moment about x was 151.5 N-m. The distal tibia (ankle) had forces of -980 N (y) and 1963 N (z), with a moment about x of 151.2 N-m.

3.5. Test 5 (Civic)

Test 4 was a good match with the actual case in terms of lower body kinematics, but the upper body motion was very different and not as close as Test 3. The WAD was much too low, and the HIC was too high. Test 5 used the same conditions because of the failure of the windshield sealant.

3.5.1. Component Trajectories

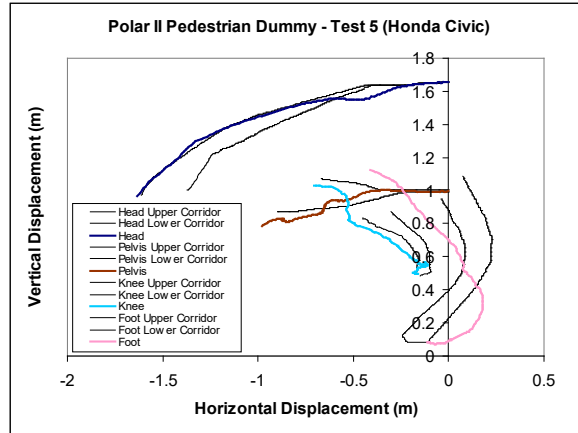


Figure 3.11. Dummy trajectories (target motion analysis) vs. PHMS corridors for similar vehicle profile

3.5.2. Overhead Path of Entire Dummy Across Vehicle Front

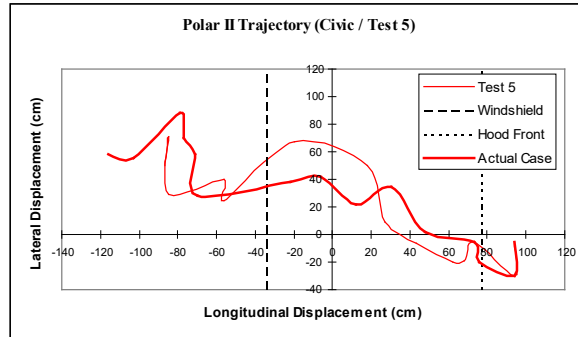


Figure 3.12. Damage patterns and comparison with marked contact points documented from actual case

3.5.3. Head

Once again, the head impacted the windshield far short of the case head contact area (WAD = 216 cm). This time, the windshield sealant did not fail. The head resultant acceleration was 495.5 g, and the calculated HIC_{36 ms} value was 3779. This was the most violent test, with the head going all the way through the windshield and impacting the steering wheel.

3.5.4. Neck

The upper neck peak forces were -986 N (y) and -3442 N (z), and the peak moment about x was 78.1 N-m. The lower neck forces were 554 N (y) and -3885 N (z), and the lower neck moment about x was -58.6 N-m. The peak front cable tensile force experienced was 727 N, and the rear cable force was 965 N. The calculated peak moment about the occipital condyle was 79.4 N-m.

3.5.5. Chest/Pelvis

The chest and pelvis resultant accelerations were 43.5 g and 74.9 g, respectively. The high pelvis acceleration could be attributed to the large amount of deformation seen in the hood.

3.5.6. Upper Leg

The femur experienced forces of -452 N (x), 751 N (y), and 4641 N (z). The moment about x was -283.6 N-m, and acceleration in the y direction on the distal medial femur was 175.3 g. The acceleration observed on the lateral side of the femur was 130.3 g. The angular acceleration calculated from these two linear accelerations was 12,847 rad/s².

3.5.7. Lower Leg

The proximal tibia experienced forces of 1909 N (x), 3341 N (y), and 3688 N (z). The moment about x was 159.8 N-m. The distal tibia (ankle) had forces of -1466 N (y) and 1923 N (z), with a moment about x of 209.3 N-m.

4. Silverado Results

4.1. Test 1 (Silverado)

The velocity was 20 km/hr. The dummy stood at a height equal to if the pedestrian were on the ground in relation to the vehicle. The arms were bent at the elbows and the legs were even with one another.

4.1.1. Component Trajectories

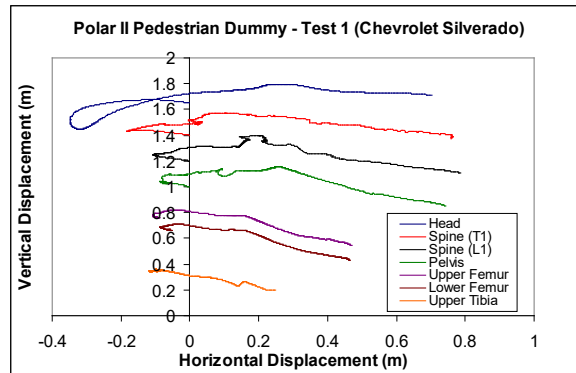


Figure 4.1. Dummy trajectories (target motion analysis) vs. PHMS corridors for similar vehicle profile

4.1.2. Overhead Path of Entire Dummy Across Vehicle Front

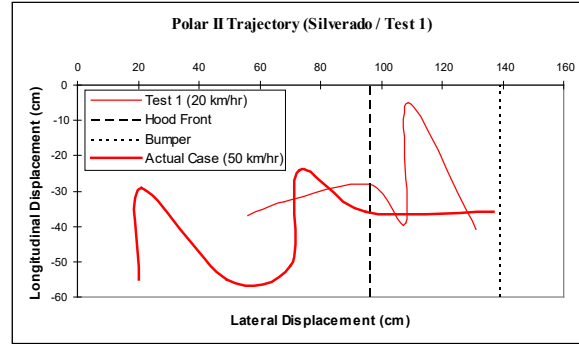


Figure 4.2. Damage patterns and comparison with marked contact points documented from actual case

4.1.3. Head

The head impacted the hood at a point corresponding to a WAD of 145. The head resultant acceleration was 84.9 g, and the calculated HIC_{36 ms} value was 284.

4.1.4. Neck

There was some minor damage to the neck segments. The upper neck peak forces were 1129 N (y) and 1523 N (z), and the peak moment about x was 83.4 N-m. The lower neck forces were 915 N (y) and 1384 N (z), and the lower neck moment about x was 125.6 N-m. The peak front cable tensile force experienced was 346 N, and the rear cable force was 182 N. The calculated peak moment about the occipital condyle was 100.9 N-m.

4.1.5. Chest/Pelvis

The chest and pelvis resultant accelerations were 29.0 g and 54.0 g, respectively. The pedestrian suffered five broken ribs in the accident, but this test was done at less than half the impact speed in the case.

4.1.6. Upper Leg

The femur experienced forces of -367 N (x), 775 N (y), and 1768 N (z). The moment about x was 396.4 N-m, and acceleration in the y direction on the distal medial femur was 132.2 g. The acceleration observed on the lateral side of the femur was 98.6 g. The angular acceleration calculated from these two linear accelerations was 12,173 rad/s².

4.1.7. Lower Leg

The proximal tibia experienced forces of 354 N (x), -930 N (y), and 1555 N (z). The moment about x was 159.8 N-m. The distal tibia (ankle) had forces of -1466 N (y) and 1923 N (z), with a moment about x of 247.4 N-m.

4.2. Test 2 (Silverado)

In test 2, the speed remained the same, but this time the right leg of the dummy was put in front of the left.

4.2.1. Component Trajectories

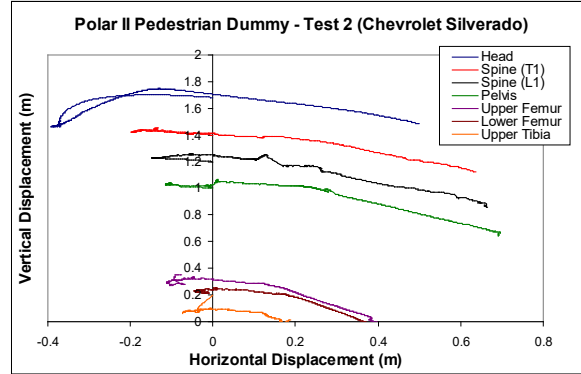


Figure 4.3. Dummy trajectories (target motion analysis) vs. PHMS corridors for similar vehicle profile

4.2.2. Overhead Path of Entire Dummy Across Vehicle Front

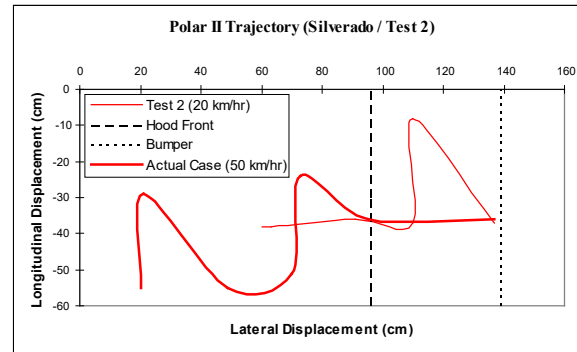


Figure 4.4. Damage patterns and comparison with marked contact points documented from actual case

4.2.3. Head

The head impacted the hood 3 cm shorter than Test 1 for a WAD of 142. The head resultant acceleration was very low once again at 101 g and the calculated HIC_{36ms} value was 334.

4.2.4. Neck

The upper neck peak forces were 983 N (y) and 1935 N (z), and the peak moment about x was 108.9 N-m. The lower neck forces were 710 N (y) and 2014 N (z), and the lower neck moment about x was 102.9 N-m. The peak front cable tensile force experienced was 448 N, and the rear cable force was 450 N. The calculated peak moment about the occipital condyle was 122.8 N-m.

4.2.5. Chest/Pelvis

The chest and pelvis resultant accelerations were 30.1 g and 53.0 g, respectively.

4.2.6. Upper Leg

The femur experienced forces of -820 N (x), 1177 N (y), and 1535 N (z). The moment about x was nearly identical to Test 1 (396.1 N-m), and acceleration in the y direction on the distal medial femur was 138.7 g. The acceleration observed on the lateral side of the femur was 103.4 g. The angular acceleration calculated from these two linear accelerations was -15,942 rad/s².

4.2.7. Lower Leg

The proximal tibia experienced forces of 299 N (x), -904 N (y), and -1692 N (z). The moment about x was 269.5 N-m. The distal tibia (ankle) had forces of -723 N (y) and 1208 N (z), with a moment about x of 103.2 N-m.

4.3. Test 3 (Silverado)

For the most part, Tests 1 and 2 were similar in forces, moments, acceleration, and trajectories. Test 3 was done at the same speed and leg position, this time with the arms folded and tied together in front.

4.3.1. Component Trajectories

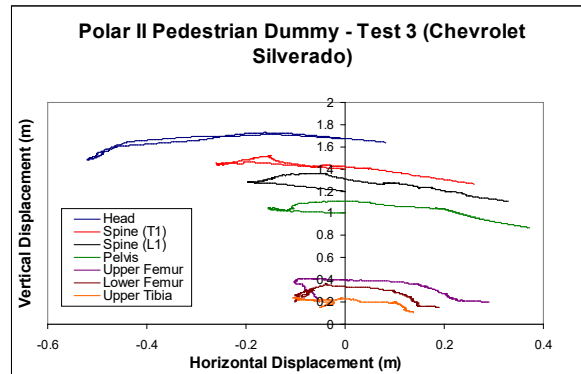


Figure 4.5. Dummy trajectories (target motion analysis) vs. PHMS corridors for similar vehicle profile

4.3.2. Overhead Path of Entire Dummy Across Vehicle Front

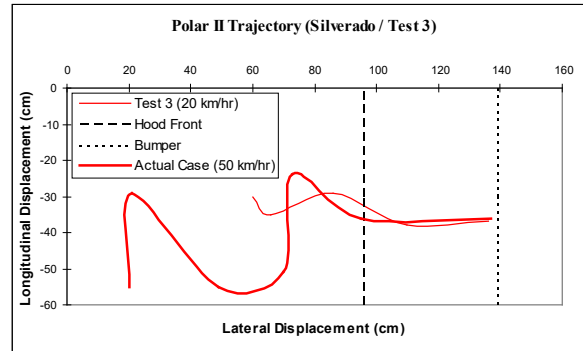


Figure 4.6. Damage patterns and comparison with marked contact points documented from actual case

4.3.3. Head

The WAD for this test was 139 cm, 3 cm shorter than in Test 2. The head resultant acceleration was 49.5 g, and the calculated $HIC_{36\text{ ms}}$ value was 207.

4.3.4. Neck

Again, as in Test 1, there was some minor damage to the neck. The upper neck peak forces were 680 N (y) and 1520 N (z), and the peak moment about x was 69.6 N-m. The lower neck forces were 707 N (y) and 1722 N (z), and the lower neck moment about x was 111.9 N-m. The peak front cable tensile force was 245 N, and the rear cable force was 119 N. The calculated peak moment about the occipital condyle was 84.1 N-m.

4.3.5. Chest/Pelvis

The chest and pelvis resultant accelerations were 26.5 g and 36.6 g, respectively.

4.3.6. Upper Leg

The femur experienced forces of -383 N (x), -1870 N (y), and 1917 N (z). The moment about x was 670.7 N-m, and acceleration in the y direction on the distal medial femur was 200.9 g. The acceleration observed on the lateral side of the femur was 137.1 g. The angular acceleration calculated from these two linear accelerations was the lowest of all tests (9,635 rad/s^2).

4.3.7. Lower Leg

The proximal tibia experienced forces of 329 N (x), -1084 N (y), and 1836 N (z). The moment about x was 293.2 N-m. The distal tibia (ankle) had forces of -824 N (y) and 1432 N (z), with a moment about x of 147.3 N-m.

4.4. Test 4 (Silverado)

The speed was increased to 25 km/hr for Tests 4 and 5, and the same dummy stance as Test 2 was used for Test 4.

4.4.1. Component Trajectories

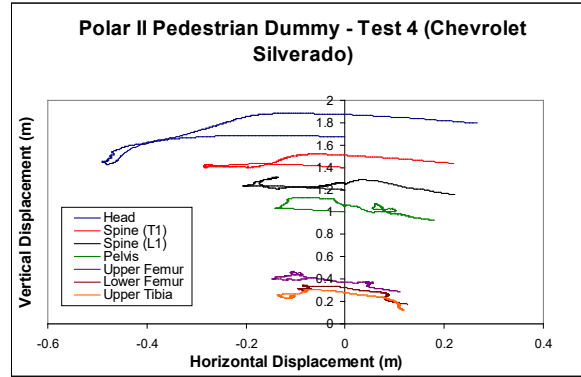


Figure 4.7. Dummy trajectories (target motion analysis) vs. PHMS corridors for similar vehicle profile

4.4.2. Overhead Path of Entire Dummy Across Vehicle Front

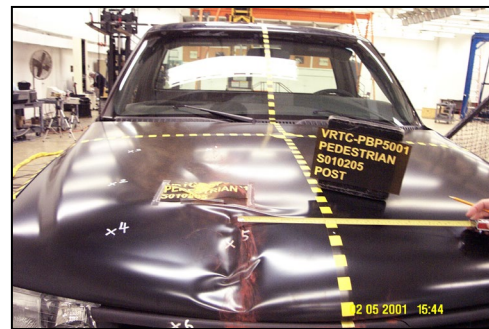
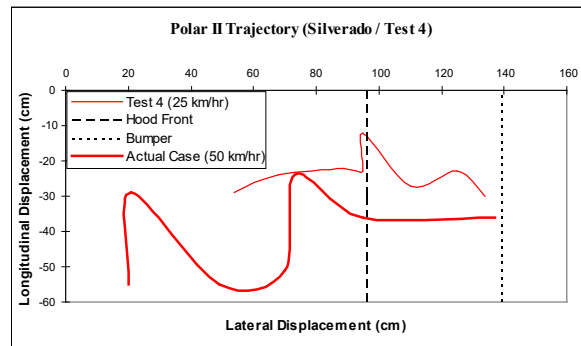


Figure 4.8. Damage patterns and comparison with marked contact points documented from actual case

4.4.3. Head

The WAD for this test was, as expected by the increase in speed, higher than all 20 km/hr tests at 149 cm. The head resultant acceleration was also significantly higher at 147.4 g, and the calculated $HIC_{36 ms}$ value was more severe (1149).

4.4.4. Neck

The upper neck peak forces were 1081 N (y) and 2269 N (z), and the peak moment about x was 51.4 N-m. The lower neck forces were 769 N (y) and 2366 N (z), and the lower neck moment about x was 121.1 N-m. The peak front cable tensile force was 232 N, and the rear cable force was 252 N. The calculated peak moment about the occipital condyle was interestingly less than lower speed tests (56.7 N-m).

4.4.5. Chest/Pelvis

The chest and pelvis resultant accelerations were 76.9 g and 138.9 g, respectively. This pelvis acceleration was the most severe out of all tests (both Civic and Silverado).

4.4.6. Upper Leg

The femur experienced forces of 579 N (x), 1475 N (y), and 2448 N (z). The moment about x was very high (770.6 N-m), and acceleration in the y direction on the distal medial femur was 195.3 g. The acceleration observed on the lateral side of the femur was 119.6 g. The angular acceleration calculated from these two linear accelerations was $-18,552 \text{ rad/s}^2$.

4.4.7. Lower Leg

The proximal tibia experienced forces of 273 N (x), -1210 N (y), and 2301 N (z). The moment about x was 284.3 N-m. The distal tibia (ankle) had forces of -810 N (y) and 1850 N (z), with a moment about x of 118.1 N-m.

4.5. Test 5 (Silverado)

Test 5 was set up to be the same as Test 3, with the hands tied together. The speed was again 25 km/hr.

4.5.1. Component Trajectories

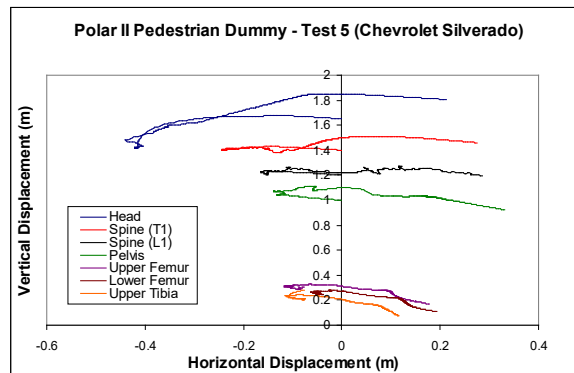


Figure 4.9. Dummy trajectories (target motion analysis) vs. PHMS corridors for similar vehicle profile

4.5.2. Overhead Path of Entire Dummy Across Vehicle Front

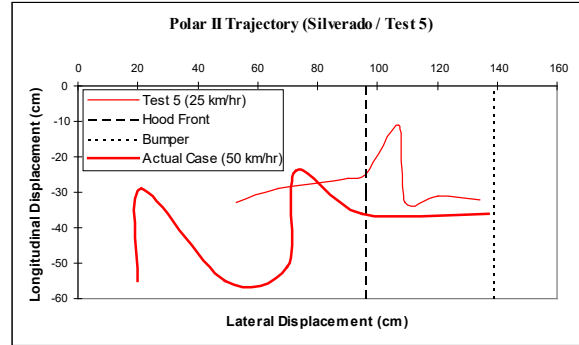


Figure 4.10. Damage patterns and comparison with marked contact points documented from actual case

4.5.3. Head

The WAD for this test was slightly lower than Test 4 (147 cm), which was the same trend noted between Tests 2 and 3 (arms at sides versus arms crossed). The head resultant acceleration was slightly lower at 141.6 g, and the calculated HIC_{36 ms} value was 1105.

4.5.4. Neck

Again, as in Tests 1 and 3, there was some minor damage to the neck. The upper neck peak forces were 1185 N (y) and 2348 N (z), and the peak moment about x was 45.9 N-m. The lower neck forces were 791 N (y) and 2560 N (z), and the lower neck moment about x was 122.3 N-m. The peak front cable tensile force was 330 N, and the rear cable force was 382 N. The calculated peak moment about the occipital condyle was 51.9 N-m.

4.5.5. Chest/Pelvis

The chest and pelvis resultant accelerations were 40.8 g and 93.4 g, respectively.

4.5.6. Upper Leg

The femur experienced forces of -578 N (x), -1653 N (y), and 2974 N (z). The moment about x was very high at 953.8 N-m, and acceleration in the y direction on the distal medial femur was 248.8 g. The acceleration observed on the lateral side of the femur was 167.6 g. The angular acceleration calculated from these two linear accelerations was very close to Test 4 (-18,524 rad/s²).

4.5.7. Lower Leg

The proximal tibia experienced forces of 324 N (x), -1420 N (y), and 2559 N (z). The moment about x was 339.6 N-m. The distal tibia (ankle) had forces of -942 N (y) and 1901 N (z), with a moment about x of 156.8 N-m.

5. Discussion

5.1. Civic Tests

For the Civic case, there were two injuries that could be directly compared with the transducer measurements from the Polar II sled tests:

- 1) Skin contusion on the left medial calf.....Upper Tibia Force
- 2) Skin avulsion on the back of the head.....Head Acceleration (HIC)

▪ Injury #1

Since our test setup was a mirror image of the case (we impacted on the left side, the case had a right side contact), the left medial calf contusion would correspond to a right medial calf contusion on the Polar dummy. Since the right leg was not instrumented, it was assumed that the medial calf was bruised from contact with either the bumper or the other leg, specifically the left knee (right knee in the case).

Dynamically, the energy transferred from the bumper to the left leg would be near the force transmitted to the right leg at contact because nothing is between both legs and the bumper. Therefore, the contact forces on the left leg and right leg were assumed to be nearly equal (Figure 5.1). Under this assumption, the upper tibia force on the left leg was compared with the injury tolerance in the literature, and this was used as the basis for determining the similarity of a test with the case.

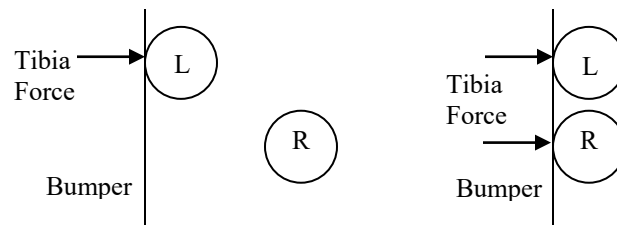


Figure 5.1. Stance does not affect force transferred to right leg

Tests 1, 2, 4, and 5 all had upper tibia forces probably too large to only cause a bruise. The forces in these tests would have likely caused knee ligament damage or fracture to the proximal tibia. Test 3 had the smallest force, but it was still above the injury threshold for a skin contusion to occur. In addition, the tests other than test 3 had femur forces high enough to cause injury to the upper leg. In the case, however, no femur injuries occurred. These comparisons indicate that test 3 was the closest match with the case for this injury.

▪ Injury #2

The injury to the head was much simpler to analyze. The head injury criterion (HIC) was the selected measure of the severity of the head impact. Based on the measurements of the head accelerometer, some conclusions could be made on the level of injury. In the case, the pedestrian suffered an AIS 1 injury (skin avulsion), which would indicate a HIC value of less than 800 [11]. Only test 3 resulted in a HIC in this range (688), indicating a high probability that the injury level simulated in the test was less than AIS 3. Extremely high HIC values in tests 1 (3088) and 5 (3779) showed a high probability of death, while tests 2 (1464) and 4 (1486) would almost certainly have resulted in severe (AIS 4-5) head injury.

▪ Kinematics

The trajectories of the head, pelvis, knee, and foot were all near the biomechanical corridors resulting from PMHS subjected to impacts from a similar vehicle profile. There was some variation between tests due to

factors such as dummy stance and initial impact point on the bumper. Correlations between things such as leg position and subsequent pedestrian kinematics would contribute greatly to the improvement of vehicle front-end design.

The maximum displacement of the head in the horizontal and vertical directions was dependent on the location of head impact on the vehicle, with Test 3 making contact closest to the case impact point. The path itself is more interesting, with Test 1 as the only one of the five where the travel of the head was within the PMHS biomechanical corridors throughout (Figure 5.2). While this was a good biofidelic comparison of the dummy, the objective was to match the case trajectory, and this test resulted in a low WAD. It seems that Test 1 drops in the vertical direction more abruptly than the other four tests, which could be a direct result of the elevation of the dummy, which was about 6 inches lower than the subsequent four tests. The impact therefore occurred closer to the center of gravity of the dummy, causing the upper body to turn downward toward the hood instead of gliding across the front of the vehicle, as was the case in Tests 2 through 4.

The relative angle between the pedestrian and vehicle did not seem to factor into the vertical and horizontal path of the head, only the overall angle of the path across the front end of the vehicle was affected. The rotation of the dummy in relation to the vehicle did initially seem to affect the head trajectory, as evidenced by Tests 2 and 3. The dummy was facing perpendicularly to the sled track in Test 2, but in the Test 3 the dummy was rotated away from the vehicle (down the track). While the head traveled in similar straight-line paths in each test (Figure 5.2), Test 3 followed the upper corridor until about one meter into the vehicle. In Test 2, however, the head trajectory was below the corridor until it crossed through at approximately one meter. The probable cause of this behavior was the complete detachment of the right leg after contact between the vehicle and pelvic area. The center of gravity was instantaneously shifted toward the upper body after loss of the leg, causing the head to be propelled further. To look directly at the effect of pedestrian orientation relative to the vehicle, we can compare Tests 2 and 4. The head traveled higher and farther in Test 4, when the dummy was rotated away from the vehicle. In Test 2, the left leg is impacted and then is sandwiched into the right leg. This results in more energy absorption in the lower body. On the other hand, in Test 4, the vehicle impacts each leg separately and more energy is transferred to the upper body (Figure 5.1), leading to a larger displacement.

Tests 4 and 5 incorporated slight differences in arm and leg positions, but nothing significant enough to change the head trajectory. The head paths in Test 4 and 5 followed roughly the same pattern, except for a noticeable “dip” in the initial stage of head movement in Test 5. This motion was most likely due to the inertia of the head moving downward prior to impact because the dummy wasn’t fully balanced prior to release of the magnet. If this did not occur, the two paths would have been close to identical.

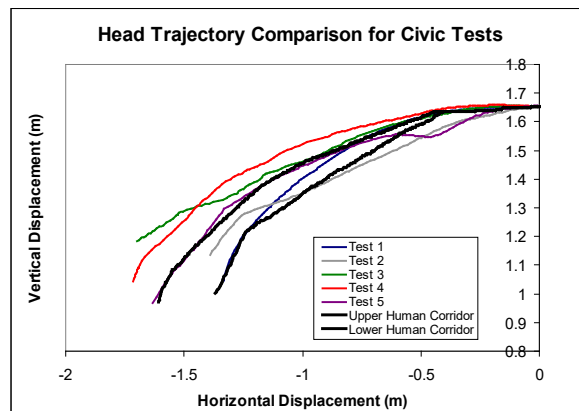


Figure 5.2. Head trajectories for all tests

The pelvis trajectories of all tests fell within the biofidelic corridors prior to 60 cm travel into the vehicle. As expected, the increase in dummy elevation increased the pelvis vertical displacement as seen in the

difference between Test 1 and Test 2 (Figure 5.3). Once again, the loss of the right leg in Test 3 caused it to have the largest horizontal displacement. A comparison of Tests 2 and 4/5 shows the effect of pedestrian orientation with the vehicle. The trajectory in Test 2 stays at roughly the same vertical position then goes up at 0.7 meters. In Tests 4 and 5, the pelvis moves in the opposite direction. An interesting extension of this study would be to look at the effect of pedestrian rotation on its kinematics.

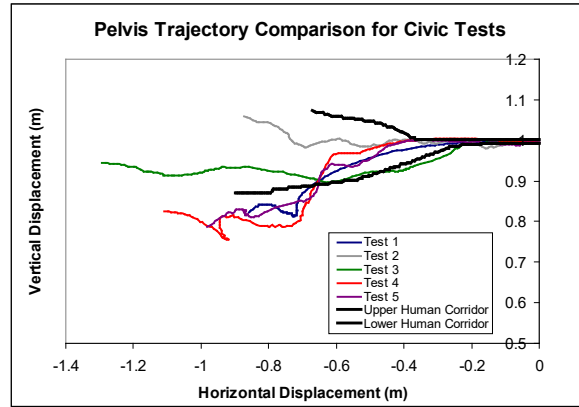


Figure 5.3. Pelvis trajectories for all tests

Unfortunately for Test 1, the knee and foot trajectory was not in view by the cameras. The views were adjusted for the next four tests, however. Test 2 had a more linear knee path when compared with the others, but for the most part, all tests showed similar trajectories (Figure 5.4). The initial knee position varied slightly, which resulted in differences in horizontal displacement. If all trajectories began at the same position, the shapes of all tests would have fallen within the corridors.

In terms of foot kinematics, Tests 2, 3, and 5 were similar for the initial 0.3 meters of horizontal displacement. Tests 3 and 5 remained similar, but Test 2 seemed to lag behind (lower horizontal position for the same vertical position) the rest of the way. It's possible that this is again due to pedestrian orientation. In Test 4, the foot began closer to the vehicle than Tests 3 and 5, which accounts for the difference in position from 3 and 5. The shapes are similar. The paths seem to turn from positive to negative horizontal displacement more abruptly than is described by the corridor. It is not clear why this is, but a reason could be that the ankle joint is too flexible.

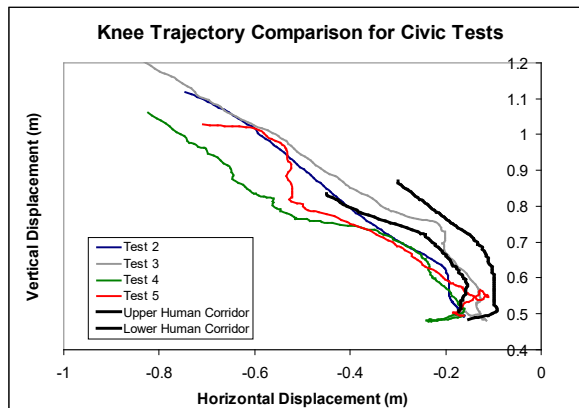


Figure 5.4. Knee trajectories for Civic tests

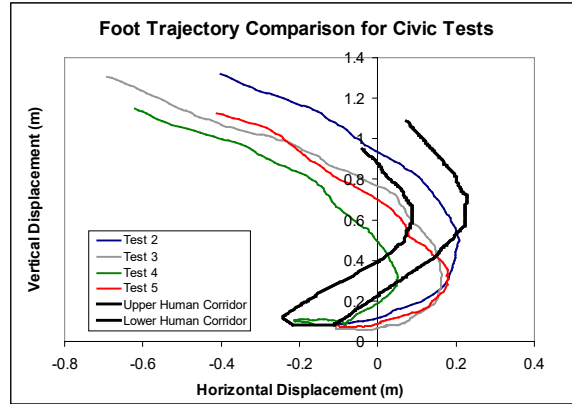


Figure 5.5. Foot trajectories for Civic tests

The wrapping of the dummy around the front end is a function of several things, including vehicle angle and speed. After Test 1, it was determined that the path up the vehicle was not at an angle similar to the case. There was quite a bit of damage to the hood of the vehicle, whereas in the case there were just some scuffs and very small dents. The vehicle was thus rotated 3 degrees, and a noticeable improvement was made in Test 2, with the lower body following the reference path very closely. The only problem was that the upper body did not travel far enough. For Test 3, as stated earlier, the dummy was positioned so that it would rotate so its back would impact the vehicle. It resulted in the best match with the case out of all tests. Test 4 showed good similarity for the lower body, but some variation to the upper body, which was due to the unpredictability of arm motion. Test 5 was also similar to the case, but the lateral displacement of the dummy near the top of the hood was up to 20 cm off. From these results, it is reasonable to assume that the pedestrian was facing away from the vehicle at impact and was elevated off the ground some distance, either as a result of jogging or jumping.

5.2. Silverado Tests

For the Silverado case, test velocities were much lower than the accident, but it was still worthwhile to extrapolate and compare injury levels with test measurements. There were seven injuries that could be analyzed:

- 1) Skin contusion on the proximal fibula.....Upper Tibia Force
- 2) Fracture of the proximal fibula.....Upper Tibia Force and Moment
- 3) Skin contusion on the left thigh.....Femur Force
- 4) Five fractured ribs (3-8).....Chest Acceleration
- 5) Bruised lung.....Chest Acceleration
- 6) Skin abrasion on temporal scalp.....Head Acceleration
- 7) Contusion on head.....Head Acceleration

▪ Injuries #1 and #2

The tibia shear force resultants (x and y directions) for all the tests were below the injury tolerance of 1600 N [12], which is to be expected because the vehicle speeds of 20 and 25 km/hr were much lower than the accident case (50 km/hr). Since there were durability concerns with the Polar dummy, testing could not be done at these high speeds with a high profile front end, such as the Silverado. In addition, the tibia force resultant (x, y, and z directions) was also below the minimum approximate force necessary to cause knee ligament damage or fracture (3840 N) [13]. The same was true for tibia bending moment about the x-axis. However, there was a dependence on impact velocity, and extrapolation of a linear relationship could give us an estimation of the forces and moments present at 50 km/hr (Figure 5.6).

Based on these estimations, there is a good probability that force and moment magnitudes associated with upper tibia injury (both fracture and skin contusion) would have occurred if testing were performed near 50 km/hr.

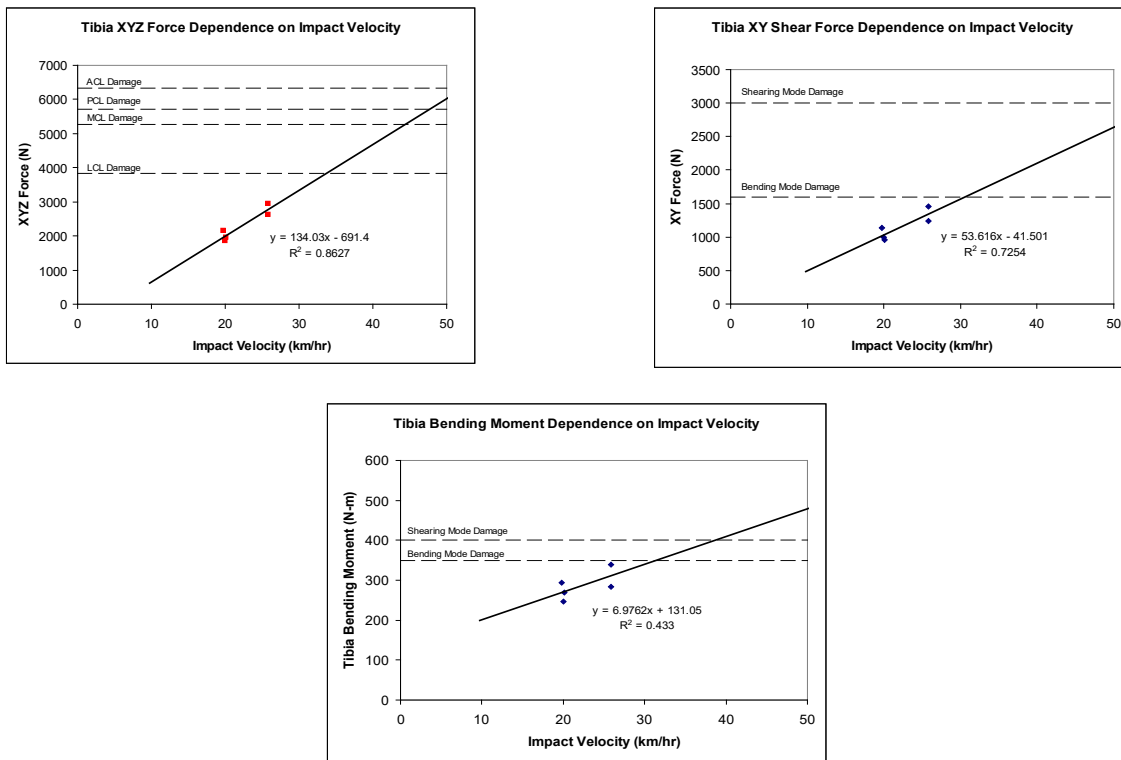


Figure 5.6. Extrapolation of test results to 50-km/hr velocity

▪ Injury #3

Based on the velocity dependence of the femur force, the pedestrian in the case was fortunate to escape with only a skin contusion on the thigh. The resultant femur force extrapolated at 50 km/hr indicates severe damage to the knee (Figure 5.7). This gives support to a nonlinear relationship between femur force and impact velocity. The trajectory of the upper body may supply more information as to why the forces were so high for low speeds. For example, the left arm may have absorbed a lot of energy prior to leg contact in the case, whereas in the tests, the leg was the first contact location. The shear force (x and y resultant) gave a trend with a very low R-squared value; therefore, it was not shown here.

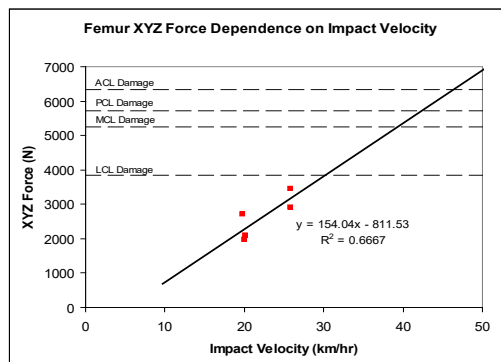


Figure 5.7. Knee force dependence on impact velocity

- Injuries #4 and #5

The pedestrian involved in the case was severely injured in the chest area, with AIS 3 (bruised lung) and AIS 4 (five fractured ribs) injuries. It was not surprising that the resultant acceleration was near the injury criteria of 67 g [14] at the low speeds of 20 and 25 km/hr. When this is extrapolated to 50 km/hr, this value was roughly three times (180 g) the injury threshold for a 50% percentile male (Figure 5.8).

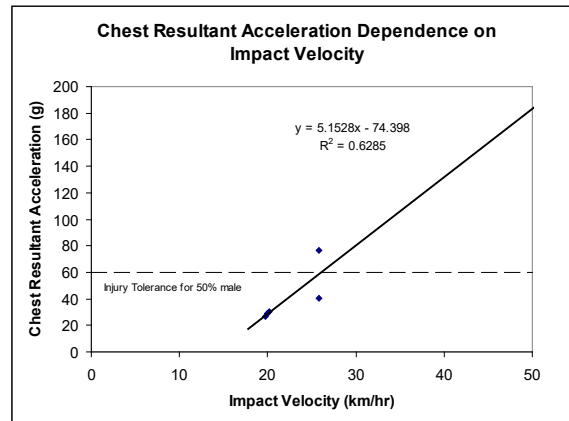


Figure 5.8. Chest acceleration extrapolated to 50 km/hr, the velocity of the case

- Injuries #6 and #7

The pedestrian received an AIS 2 contusion on the back of the head. This is consistent with a HIC of below 800. For the Silverado tests at 20 km/hr, this was the case. The average HIC at this speed was 275 (n=3). As expected, there is a definite relationship between HIC and velocity, with the average HIC at 25 km/hr at 1127 (n=2). This indicates that the dummy was in the serious head injury range already at 25 km/hr. Based on an assumed linear relationship between HIC and velocity, the pedestrian would have been fatally injured at 50 km/hr (Figure 5.9).

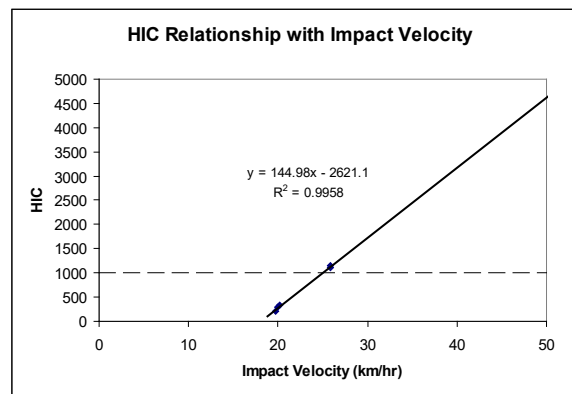


Figure 5.9. Head injury criterion

The estimated HIC at 50 km/hr is extremely high when compared with the pedestrian injuries suffered in the actual case. One reason may have to do with the flexibility of the shoulder. If the shoulder is too stiff, it may not absorb enough energy at impact, and this energy is transmitted to the neck and subsequently the head. This condition could lead to a high neck moment and speed, causing the head to strike the vehicle at a high speed. Another reason could be the flexibility of the neck itself. If it is too flexible, it will not

sufficiently resist movement of the head, again leading to an excessive head speed. There were indications after the first 25 km/hr test that the neck was becoming fatigued, noted by small fissures between the rubber and steel segments. This would certainly increase flexibility. Finally, the speed of the vehicle at impact affects the wrap around distance (WAD). This measure gives the location of head impact up the front of the vehicle. The greater the speed of the vehicle is, the greater the WAD. A higher speed could cause the duration of contact with the upper body (arm, thorax, shoulder) to increase, which would increase energy absorption prior to head contact and maybe even prevent contact with the hood. The WAD, by definition, determines the location of the hood where the head makes contact. It has been shown that head impact severity is based in part by the hood reinforcement and underhood clearance [15]. It's possible that the pedestrian's head in the case impacted a non-reinforced, high clearance area of the hood, which would result in a low HIC. On the other hand, the dummy's head contacted a reinforced, low clearance region, giving a higher HIC at a lower speed.

- Kinematics

The influence of velocity and dummy stance on the motion of the head was the major issue in this series of tests. Pedestrian trajectories in response to a higher-profile vehicle impact are not believed to be available in the literature. These tests will hopefully give insight into this behavior, and possibly even establish some approximate corridors for pedestrian motion based on good dummy biofidelity observed in the Civic tests.

Velocity did have an effect on the horizontal displacement of the head, with the 25-km/hr tests resulting in higher translations (Figure 5.10). It should be noted that for Test 3, a backup camera was used for trajectory analysis, resulting in a different angle and a head motion not consistent with the other four tests. For Tests 1 and 2 (20 km/hr), the average horizontal displacement was 0.37 meters from the initial position. For Tests 4 and 5 (25 km/hr), this magnitude was 0.46 meters, an increase of 9 cm.

The arm and leg positions were varied for these tests, causing more changes in kinematics. For Test 1, the legs were in line and the arms were bent at the elbows with the hands free. In Test 2, the right leg was in front of the left and the arms were in the same position as Test 1. This change in leg position resulted in a higher trajectory of the head and subsequent increase of 4 cm in horizontal translation. In Test 4, the same stance as Test 2 was applied, this time at a higher speed. In Test 5, the same leg position was applied as in Test 4, but the hands were tied together. This resulted in a lower translation (5 cm) than in Test 4, most likely because the arms were closer to the body and therefore the head did not have as far to travel for impact with the hood.

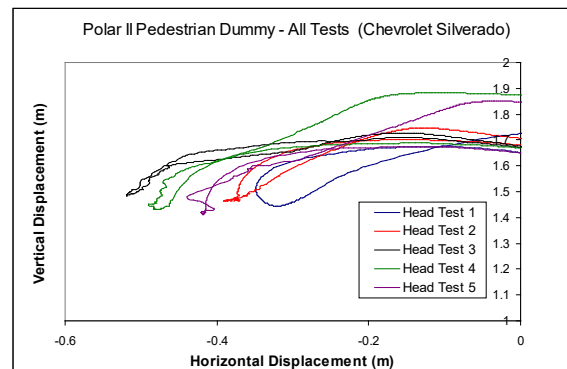


Figure 5.10. Motion of the head in the Silverado tests

5.3. Durability

Several dummy components were damaged during the test series, especially in the Civic portion because of the high velocity testing. In Test 1 (Civic), the left shoulder shaft was sheared because of what looked like a direct compressive blow to the elbow that occurred near the border of the windshield frame, which is very

stiff (Figure 5.11). It was unknown whether this type of fracture had occurred previously, but if not, fatigue may have played a part.



Figure 5.11. Left shoulder shaft fracture

In Test 2, several components were damaged. The rear neck cable snapped from excessive tension, leading to less restriction of neck motion and cracking of the segments. The high force associated with cable failure was after the head had penetrated the windshield (Figure 5.12).



Figure 5.12. Circumstances leading to rupture of the rear neck cable

The pelvis resultant acceleration was not extremely high in Test 2, but there was damage to the lumbar flex joint. It was thus concluded that the damage was due to fatigue for the most part. Some of the internal sensor cables were tied loosely to the flex joint, which may have caused more stress. In Test 3, the right proximal femur was fractured and the entire right leg was detached (Figure 5.13).



Figure 5.13. Fracture of the right hip joint

Overall, the damage to the dummy was minimal considering the violent nature of the tests. The legs held up well. The left tibia was replaced prior to each Civic test and was not damaged during the entire series. The major problems occurred in the neck. A recommended change would be at the interface of the rubber and steel segments. The relative stiffness of these parts contributes to high stress concentration and subsequent cracking. A change in materials or assembly method should increase the fatigue life of the neck for future testing.

5.4. Sled Buck

The buck served its purpose and performed without incident, except for some vibration during the Silverado testing. This vertical vibration was due to the large amount of weight cantilevered off to the side. Some dynamic analysis would be helpful in determining structural modifications that would reduce this vibration. One recommendation would be to build the buck up vertically with angled members attached to the center of the sled. Another would be to attach rollers or wheels to the four corners of the buck.

6. Conclusions/Recommendations

This study was encouraging in that a biofidelic test device will soon be available for testing automobile aggressiveness toward pedestrians. The behavior of the dummy was near biomechanical corridors for the Civic tests, and it held up under high velocity conditions. In terms of reconstructing cases with the Polar dummy, it seems that we can get close to what happened in the accident, but it will be very difficult to match a case exactly by using the dummy. One of the tests (Test 3) was very close to replicating damage patterns and head/leg measurements indicative of the injuries suffered by the pedestrian. However, two tests with the same conditions had very different results. Before we can become efficient in reconstructing cases, it is necessary to become more familiar with the conditions of dummy stance/orientation, vehicle rotation, and velocity and how they affect pedestrian kinematics. The only way to accomplish this is to perform a great number of tests, which could more easily be done with computer simulations once a pedestrian model is established. The more tests done in different configurations, the more knowledgeable we will become in terms of understanding the pedestrian/vehicle collision environment. Once it is known, for instance, that if the legs are a certain distance apart, the head will travel in a certain path. Perhaps the cost of using a pedestrian dummy would be too much when compared to using component test procedures, but tests with a PMHS-validated dummy could provide valuable information toward an accurate pedestrian computer model. Thousands of different vehicle/pedestrian interactions could then be simulated in a very efficient manner, which would lead to a better understanding of the parameters that dictate pedestrian response.

7. References

1. Schneider H, Beier G, "Experiment and Accident: Comparison of Dummy Test Results and Real Pedestrian Accidents," SAE 741177, Eighteenth Stapp Car Crash Conference Proceedings: 29-69.
2. Pritz HB, Hassler CR, Herridge JT, Weis EB, "Experimental Study of Pedestrian Injury Minimization Through Vehicle Design," SAE 751166, Nineteenth Stapp Car Crash Conference Proceedings: 725-751.
3. Stcherbatcheff G, Tarriere C, Duclos P, Fayon A, "Simulation of Collisions Between Pedestrians and Vehicles Using Adult and Child Dummies," SAE 751167, Nineteenth Stapp Car Crash Conference Proceedings: 753-785.
4. Bacon GC, Wilson MR, "Bumper Characteristics for Improved Pedestrian Safety," SAE 760812, Twentieth Stapp Car Crash Conference Proceedings: 391-428.
5. Krieger KW, Padgaonkar AJ, King AI, "Full-Scale Experimental Simulation of Pedestrian-Vehicle Impacts," SAE 760813, Twentieth Stapp Car Crash Conference Proceedings: 431-463.
6. Pritz HB, "Comparison of the Dynamic Responses of Anthropometric Test Devices and Human Anatomic Specimens in Experimental Pedestrian Impacts," SAE 780894, Twenty-second Stapp Car Crash Conference Proceedings: 343-357.
7. Ravani B, Brougham D, Mason RT, "Pedestrian Post-Impact Kinematics and Injury Patterns," SAE 811024, Twenty-fifth Stapp Car Crash Conference Proceedings: 791-822.
8. Yoshida S, Akiyama A, Matsuhashi T, Rangarajan N, Shams T, Ishikawa H, Konosu A, "Development of Simulation Model and Pedestrian Dummy," SAE Document No. 1999-01-0082, International Congress & Exposition, Detroit, MI, March 1999.
9. Isenberg, R.A., Chidester, C., Mavros, S.; "Update on the Pedestrian Crash Data Study," Sixteenth International Technical Conference on the Enhanced Safety of Vehicles, Paper No. 98-S6-O-05, 1998.
10. Padgaonkar AJ, et al, "Measurement of Angular Acceleration of a Rigid Body using Linear Accelerometers," J Appl Mech, 42 (1975): 552-556.
11. McIntosh AS, Kallieris D, Mattern R, Miltner E, "Head and Neck Injury Resulting from Low Velocity Direct Impact," SAE 933112, Thirty-seventh Stapp Car Crash Conference Proceedings: 43-57.
12. Kajzer J, Schroeder G, Ishikawa H, Matsui Y, Bosch U, "Shearing and Bending Effects at the Knee Joint at High Speed Lateral Loading," SAE 973326, Forty-first Stapp Car Crash Conference Proceedings: 151-165.
13. Yang J, Kajzer J, Cavallero C, Bonnolt J, "Computer Simulation of Shearing and Bending Response of the Knee Joint to a Lateral Impact," SAE 952727, Thirty-ninth Stapp Car Crash Conference Proceedings: 251-264.
14. Cavanaugh JM, Walilko TJ, Malhotra A, Zhu Y, King AI, "Biomechanical Response and Injury Tolerance of the Thorax in Twelve Sled Side Impacts," SAE 902307, Thirty-fourth Stapp Car Crash Conference Proceedings: 23-38.
15. Stammen JA, Saul RA, Ko B, "Pedestrian Head Impact Testing and PCDS Reconstructions," Seventeenth International Technical Conference on the Enhanced Safety of Vehicles (2001).
16. Mertz HJ, Patrick LM, "Strength and Response of the Human Neck," SAE 710855, Fifteenth Stapp Car Crash Conference Proceedings.

17. Voo LM, Pintar FA, Yoganandan N, Liu YK, "Static and Dynamic Bending Responses of the Human Cervical Spine," *J Biomech Eng* (1998); 120(6): 693-699.
18. Pintar FA, Yoganandan N, Voo L, Cusick JF, Maiman DJ, Sances A, "Dynamic Characteristics of the Human Cervical Spine," *SAE 952722*, Thirty-ninth Stapp Car Crash Conference Proceedings: 195-202.
19. Cheng R, Yang KH, Levine RS, King AI, Morgan R, "Injuries to the Cervical Spine caused by a Distributed Frontal Load to the Chest," *SAE 821155*, Twenty-sixth Stapp Car Crash Conference Proceedings: 1-40.
20. Tarriere C, Walfisch G, Fayon A, Rosey JP, Got C, Patel A, Delmus A, "Synthesis of Human Tolerances Obtained from Lateral Impact Simulations," *Seventh International Technical Conference on the Enhanced Safety of Vehicles* (1979): 359-373.
21. Zhu JY, Cavanaugh JM, King AI, "Pelvic Biomechanical Response and Padding Benefits in Side Impact Based on a Cadaveric Test Series," *SAE 933128*, Thirty-seventh Stapp Car Crash Conference Proceedings: 223-233.
22. Cavanaugh JM, Walilko TJ, Malhotra A, Zhu Y, King AI, "Biomechanical Response and Injury Tolerance of the Pelvis in Twelve Sled Side Impacts," *SAE 902305*, Thirty-fourth Stapp Car Crash Conference Proceedings: 1-12.
23. Crandall JR et al, "Biomechanical Response and Physical Properties of the Leg, Foot, and Ankle," *SAE 962424*, Fortieth Stapp Car Crash Conference Proceedings: 173-192.

8. Appendix

8.1. Summary table of peak data

Test Date	1999 Honda Civic					1999 Chevrolet Silverado				
	1/24/01	1/25/01	1/29/01	1/29/01	1/31/01	2/1/01	2/2/01	2/2/01	2/5/01	2/6/01
Raw File	389	390	391	392	393	396	397	398	401	402
Vehicle Angle (degrees from center)	17	20	20	20	20	0	0	0	0	0
Impact Velocity (km/hr)	48.62	48.75	48.44	48.44	48.24	20.00	20.14	19.77	25.86	25.86
Impact Velocity (mph)	30.21	30.29	30.10	30.10	29.98	12.43	12.51	12.29	16.07	16.07
Head X Acceleration (g)	98.46	-166.06	92.91	277.88	-454.71	-11.76	-16.91	-9.69	43.26	35.38
Head Y Acceleration (g)	372.57	83.24	70.78	215.95	263.79	82.59	100.22	45.78	141.27	139.22
Head Z Acceleration (g)	105.34	77.41	43.22	85.90	137.15	34.89	42.39	35.75	52.93	51.51
Upper Neck Y Force (N)	-2364.69	-950.78	-951.30	-583.34	-985.56	1128.75	982.53	680.45	1080.96	1185.20
Upper Neck Z Force (N)	3938.76	3137.94	-2855.98	2572.19	-3442.49	1523.45	1935.08	1519.84	2268.80	2347.86
Upper Neck X Moment (N-m)	71.93	-65.78	-31.21	40.70	78.13	83.39	108.87	69.60	51.41	45.85
Lower Neck Y Force (N)	-2411.39	1439.94	749.34	658.14	553.85	914.82	710.30	706.88	769.37	790.82
Lower Neck Z Force (N)	4382.19	3135.10	-3031.12	2483.15	-3885.09	1383.93	2014.32	1722.29	2366.07	2560.45
Lower Neck X Moment (N-m)	-95.12	-84.45	-72.39	-64.69	-58.56	125.56	102.88	111.85	121.16	122.26
Neck Front Cable Z Force (N)	603.85	603.02	226.00	674.96	726.50	345.51	448.17	244.63	232.19	329.93
Neck Rear Cable Z Force (N)	1175.36	3361.27	480.25	101.34	965.12	182.15	450.23	119.37	251.61	381.52
Chest X Acceleration (g)	-21.08	-36.27	63.99	27.39	37.85	7.95	18.76	13.96	27.19	16.80
Chest Y Acceleration (g)	55.69	62.11	21.19	32.64	23.29	28.90	29.29	25.66	76.45	39.78
Chest Z Acceleration (g)	37.81	28.87	24.57	23.09	19.44	12.24	9.73	9.32	14.92	15.70
Left Femur X Force (N)	1216.46	581.44	555.24	638.48	-451.65	-367.48	-819.67	-382.53	578.59	-578.07
Left Femur Y Force (N)	-947.11	545.45	-880.89	732.71	750.52	774.55	1176.75	-1869.81	1474.75	-1653.46
Left Femur Z Force (N)	5854.19	5223.53	3520.24	5044.65	4641.06	1767.99	1535.45	1916.93	2447.50	2973.95
Left Femur X Moment (N-m)	-277.72	-209.81	-226.43	-228.32	-283.59	396.44	396.08	670.72	770.63	953.76
Left Femur Proximal Lateral Y Acceleration (g)	222.77	-174.60	102.54	108.91	130.34	98.59	103.42	137.10	119.59	167.63
Left Femur Distal Medial Y Acceleration (g)	287.86	-236.10	138.43	131.77	175.27	132.17	138.65	200.87	195.26	248.75
Left Upper Tibia X Force (N)	1658.96	2391.70	2982.34	2904.50	1909.13	353.93	298.76	329.32	272.72	323.67
Left Upper Tibia Y Force (N)	807.74	2264.11	2534.33	2709.48	3340.95	-930.42	-904.12	-1084.47	-1209.56	-1420.22
Left Upper Tibia Z Force (N)	5048.58	4781.77	2564.78	3836.27	3688.43	1554.58	-1692.91	1836.01	2301.17	2558.97
Left Upper Tibia X Moment (N-m)	124.47	126.66	188.41	151.50	159.82	247.41	269.48	293.19	284.30	339.60
Left Lower Tibia Y Force (N)	-656.09	-1329.20	-1194.49	-980.22	-1465.97	-809.68	-723.08	-824.21	-810.34	-941.79
Left Lower Tibia Z Force (N)	3281.23	2068.72	2411.17	1962.74	1923.42	1368.14	1208.23	1431.97	1850.13	1901.04
Left Lower Tibia X Moment (N)	105.32	120.11	115.40	151.22	209.30	119.97	103.20	147.28	118.10	156.84
Left Tibia Proximal Lateral Y Acceleration (g)	332.69	-317.93	-393.22	182.08	-377.47	-377.47	112.70	213.10	-382.65	256.60
Left Tibia Distal Medial Y Acceleration (g)	336.02	-245.18	154.12	177.19	245.04	180.52	100.49	185.00	130.75	214.71
Pelvis X Acceleration (g)	-46.52	-47.40	95.52	44.58	57.37	-29.87	-40.65	-13.38	-132.25	-58.53
Pelvis Y Acceleration (g)	45.17	34.96	-90.07	37.10	46.78	43.80	51.70	35.46	69.54	88.40
Pelvis Z Acceleration (g)	-32.69	-30.43	46.55	-21.88	-23.82	-13.75	-15.25	-12.76	35.87	47.81

8.2. Summary table of calculations

Test Date	1999 Honda Civic					1999 Chevrolet Silverado				
	1/24/01	1/25/01	1/29/01	1/29/01	1/31/01	2/1/01	2/2/01	2/2/01	2/5/01	2/6/01
Raw File	389	390	391	392	393	396	397	398	401	402
Vehicle Angle (degrees from center)	17	20	20	20	20	0	0	0	0	0
Impact Velocity (km/hr)	48.62	48.75	48.44	48.44	48.24	20.00	20.14	19.77	25.86	25.86
Impact Velocity (mph)	30.21	30.29	30.10	30.10	29.98	12.43	12.51	12.29	16.07	16.07
Head Resultant Acceleration (g)	373.61	168.70	109.92	352.51	495.47	84.90	101.03	49.51	147.38	141.63
HIC (15 ms)	3088	1229	573	1346	3779	231	193	113	1149	1105
HIC (36 ms)	3088	1464	688	1486	3779	284	334	207	1149	1105
Neck Moment about the Occipital Condyle (N-m)	51.90	-76.39	-36.59	41.69	79.38	100.94	122.77	84.10	56.70	51.85
Nij	0.747	0.793	0.510	0.461	0.722	0.395	0.472	0.343	0.461	0.416
Net	0.747	0.642	0.350	0.428	0.492	0.332	0.362	0.287	0.461	0.409
Nec	0.462	0.793	0.510	0.400	0.550	0.089	0.339	0.215	0.259	0.287
Nft	0.671	0.441	0.178	0.194	0.167	0.395	0.472	0.343	0.434	0.416
Nfc	0.641	0.549	0.096	0.461	0.722	0.324	0.062	0.303	0.101	0.074
Chest Resultant Acceleration (g)	60.68	66.23	67.22	42.30	43.48	28.98	30.14	26.45	76.89	40.76
Pelvis Resultant Acceleration (g)	54.98	56.50	115.48	45.21	74.91	54.00	53.05	36.56	138.86	93.41
Femur Angular Acceleration (rad/s ²)	16474	-32338	15643	11466	12847	12173	-15942	9635	-18552	-18524
Tibia Angular Acceleration (rad/s ²)	-32226	25787	Bad	24353	Bad	Bad	-12854	21991	Bad	-17280
Wrap Around Distance (cm)	182	222	239	217	216	145	142	139	149	147
Arms	2	2	2	2	2	2	2	1	2	1
Legs	1	1	3	3	3	1	2	2	2	2
Broken Dummy Components	1	2,3,4	5	---	---	3 (sg)	---	3 (sg)	---	3

Arms:

1. Even
2. At Sides

Legs:

1. Even
2. Right in front of Left
3. Left in front of right

Broken Dummy Components:

1. Fractured Left Shoulder Shaft
2. Torn Rear Neck Cable
3. Cracked Neck Segments
4. Cracked Lumbar Joint
5. Fractured Right Hip Joint

sg - superglue used to repair

8.3. Injury tolerances

Injury	Tolerance Level	Reference
Head Injury Criteria (HIC)	< 800 (AIS 1-2), >1000 (serious injury)	11
Equivalent Neck Moment about Occipital Condyle (Flexion)	88 N-m	16
Equivalent Neck Moment about Occipital Condyle (Extension)	47 N-m	16
Neck Shear Failure Force	845 N	16
Neck Compressive Failure Force	3055 +/- 267 N	17
	3326 N	18
Neck Resultant Force	6200 N	19
Chest Acceleration (square of sum of squares of x and y)	66.9 g (25% prob of AIS 4 or greater)	14
	133.2 g (TT1, 25% prob of AIS 4)	14
Pelvic Resultant Acceleration	62 g	20
	49 g	21
Pelvic Force	5000 N (25% probability)	21
	8000 N (25% probability)	22
Anterior Cruciate Ligament (ACL) Rupture Force	6330 N	13
Posterior Cruciate Ligament (PCL) Rupture Force	5710 N	13
Lateral Collateral Ligament (LCL) Rupture Force	3840 N	13
Medial Collateral Ligament (MCL) Rupture Force	5260 N	13
Tibia/Femur Bending Moment at Knee Injury	400 - 500 N-m (Shear)	12
	350 - 400 N-m (Bending)	12
Tibia/Femur Shear Force at Knee Injury	3000 N (Shear)	12
	1600 N (Bending)	12
Ankle Moment	60 N-m	23
Achilles Tendon Rupture Force	1000 - 1500 N	23

8.4. Accident case injuries and transducers used for comparison

Civic Injuries

Body Region	Type of Anatomic Structure	Specific Anatomic Structure	A.I.S. Severity	Injury Source	Type of Damage	Damage Depth	Transducer	
Medial Left Calf	Skin	Contusion	1	Front Bumper	Scuff	Surface only	Upper Tibia Fx, Fy, Fz	
Dorsal Right Middle Ring and Little Finger	Skin	Avulsion	1	Windshield	Cracked	Crush 2-5 cm		
Right Wrist	Skin	Laceration	1	Windshield	Cracked	Crush 2-5 cm		
Right Forearm	Skin	Abrasion	1	Windshield	Cracked	Crush 2-5 cm		
Right Forearm	Skin	Laceration	1	Windshield	Cracked	Crush 2-5 cm		
Left Upper Arm	Skin	Laceration	1	Windshield	Cracked	Crush 2-5 cm		
Head	Skin	Avulsion	1	Windshield	Cracked	Crush 2-5 cm		Head Accel Head Accel
Head	Skin	Laceration	1	Windshield	Cracked	Crush 2-5 cm		
Right Forearm	Skin	Laceration	1	Windshield	Cracked	Crush 0-2 cm		
Face	Skin	Abrasion	1	Ground	Not from Vehicle	Not from Vehicle		

Silverado Injuries

Body Region	Type of Anatomic Structure	Specific Anatomic Structure	A.I.S. Severity	Injury Source	Type of Damage	Damage Depth	Transducer
Proximal Fibula	Skin	Contusion	1	Front Bumper	No Damage	No Damage	Upper Tibia Fx, Fy, Fz
Proximal Fibula	Skeletal	Fracture	2	Front Bumper	No Damage	No Damage	
Left Thigh	Skin	Contusion	1	Front Grill	Cracked	Crush 2-5 cm	Femur Fx, Fy, Fz
Middle Left Upper Arm	Skin	Contusion	1	Hood Edge	Dent	Crush 2-5 cm	
Proximal Humerus	Skeletal	Fracture	2	Hood Edge	Dent	Crush 2-5 cm	
3rd through 8th Ribs	Skeletal	Fracture	4	Hood Edge	Dent	Crush 2-5 cm	Chest Accel Chest Accel
Lung	Organs	Contusion	3	Hood Edge	Dent	Crush 2-5 cm	
Nose	Skin	Contusion	1	Hood Surface	Dent	Crush 0-2 cm	Head Accel Head Accel
Temporal Scalp	Skin	Abrasion	1	Hood Surface	Dent	Crush 0-2 cm	
Head	Head	Contusion	2	Hood Surface	Dent	Crush 0-2 cm	
Right Occipital Scalp	Skin	Laceration	1	Ground	Not from Vehicle	Not from Vehicle	

8.5. Dummy stance dimensions

Test Number	Car	1	2	3	4	5	1	2	3	4	5	
		Honda Civic					Chevy Silverado					
Speed		50 kph (30mph)					20 kph (12.5 mph)		25 kph (15.6 mph)			
Angle		17 deg	20 deg	20 deg	20 deg	20 deg	0 deg	0 deg	0 deg	0 deg	0 deg	
Units		Inches	Inches	Inches	Inches	Inches	Inches	Inches	Inches	Inches	Inches	
1	Heel to Heel	13.5	13.0	14.5	13.0	14.3	14.5	17.5	16.3	16.0	16.0	
2	Toe to Toe	14.8	14.0	19.0	18.0	18.8	15.8	16.8	16.8	16.8	17.0	
3	Right Knee	Height	19.8	19.8	21.3	19.8	20.8	20.8	20.5	20.3	21.0	20.5
		Lead	6.5	6.3	4.5	5.0	4.5	3.3	3.5	3.5	3.5	4.0
	Left Knee	Height	19.3	19.3	21.0	20.3	20.8	20.3	20.5	21.3	20.5	21.3
		Lead	7.5	7.5	5.0	4.5	6.0	4.0	5.0	4.0	4.5	4.5
4	Knee to Knee	12.0	11.5	12.5	10.8	11.0	11.5	12.0	11.5	11.5	11.8	
5	Angle to Condyle [deg]	Right	3.5	0.5	2.5	14.0	4.0	6.0	17.0	14.0	12.0	13.0
		Left	6.5	2.5	4.0	11.0	5.0	0.5	9.0	3.5	7.5	2.5
6	Pelvis Bolt to Heel	Height	36.5	37.5	35.8	37.5	38.3	38.3	37.5	38.3	37.0	37.5
		Lead	6.5	4.8	4.5	2.3	3.5	2.0	2.0	0.0	2.3	2.0
7	Pubic Symph to Heel	Right	3.4	5.0	3.5	47.0	5.5	5.8	6.0	5.5	5.5	5.5
		Left	6.0	5.0	5.3	4.0	5.0	6.0	6.5	6.5	5.3	6.0
8	Pelvis to Lumbar Bolt	Height	n/a	n/a	n/a	n/a	n/a	n/a	n/a	n/a	n/a	n/a
		Lead	n/a	n/a	n/a	n/a	n/a	n/a	n/a	n/a	n/a	n/a
9	Pelvis to Neck Surface	Height	19.0	18.8	21.3	21.8	21.3	20.3	21.3	21.3	20.8	21.0
		Lead	0.0	0.0	0.0	2.5	0.0	1.0	1.0	2.5	2.0	2.8
10	Head CG	Height	63.8	63.8	64.3	65.5	65.8	70.0	70.5	70.3	70.0	69.8
11	Arm Angle-Forward [deg]	Right	(-) 9.0	(-) 9	(-) 15	(-) 27	(-) 15.5	(-) 6.5	(-) 5.5	(-) 7.5	(-) 5.5	(-) 7
		Left	(-) 7.0	(-) 7	14.0	17.0	14.2	(-) 8	(-) 5.5	(-) 1.6	(-) 6	(-) 2
12	Elbow Width	18.3	17.8	20.3	20.5	20.0	18.0	19.3	18.8	20.5	19.5	
13	Arm Angle-Side [deg]	Right	(-) 10	(-) 10.5	(-) 16	19.0	(-) 15.2	(-) 9.0	(-) 12.0	(-) 3.0	(-) 12.3	(-) 4
		Left	(-) 7	(-) 8	(-) 8.5	12.0	12.0	(-) 7.0	(-) 9.0	(-) 7.0	(-) 9.5	(-) 6
14	Dist. From side Cam. To Dum (Perpendicular Distance)	139.0	187.0	190.0	192.0	191.0	174.0	173.0	174.0	172.0	171.0	
		137.0	185.0	188.0	189.0	184.0	156.0	168.0	154.0	155.0	154.0	
15	Dist. From Ovhd Cam to Ground	208.0	208.0	208.0	208.0	208.0	208.0	208.0	208.0	208.0	208.0	
16	Dist. From Bumper to Dum	50.5	51.0	52.5	54.0	51.8	11.3	11.5	12.0	20.0	20.5	
17	Dist. From Vehicle to SideCam (Perpendicular Distance)	159.0	203.0	204.0	204.0	201.0	177.0	177.0	176.0	174.0	176.0	
		148.0	160.0	197.0	169.0	191.0	140.0	140.0	139.0	137.0	139.0	
18	Flour to Top of Dum	78.8	85.5	84.5	85.0	84.5	73.0	72.8	73.5	72.8	73.5	
19	Height of Elevation	10.6	17.0	16.0	17.0	16.3	4.8	4.5	4.5	4.8	4.8	

Civic:

Distance between Ground to Top surface of Bumper : 32.09 in
 Distance between Side camera to Reference point : 176 in

Silverado:

Distance between Ground to Top surface of Bumper : 36.25 in
 Distance between Side camera to Reference point : 163 in

8.6. Transducer list (vendor, S/N, model, etc.)

*(signal voltage/excitation voltage)

Location	Transducer	Dir	Sensor Polarity Check	Serial Number	Serial Number	Input Resistance Ω	Output Resistance Ω	Sensitivity	unit*
Head	Triaxial Accel.	x	back	ENDEVCO 7264-2000	J32068	1309	1323	0.02608	(mV/V)/g
		y	right	ENDEVCO 7264-2000	J28382	1485	1488	0.02343	(mV/V)/g
		z	bottom	ENDEVCO 7264-2000	J28644	1367	1375	0.02486	(mV/V)/g
Neck	Upper LC	fy	topsurface - left	DENTON 3454	81	349	349	0.0002322	(mV/V)/N
		fz	tension	DENTON 3454	81	698	697	0.00008364	(mV/V)/N
		mx	topsurface - front	DENTON 3454	81	349	349	0.005852	(mV/V)/Nm
	Lower LC	fy	topsurface - left	DENTON 2357	82	349	350	0.000174	(mV/V)/N
		fz	tension	DENTON 2357	82	700	700	0.00007115	(mV/V)/N
		mx	topsurface - front	DENTON 2357	82	349	349	0.004076	(mV/V)/Nm
	Fr. Spring LC	cable	cable tension (-)	ENDEVCO 7264-2000	122247	350	350	0.0003041	(mV/V)/N
Rr. Spring LC	cable	cable tension(+)	ENDEVCO 7264-2000	122248	350	350	0.0002808	(mV/V)/N	
Thorax	Triaxial Accel.	x	back	ENDEVCO 7264-2000	J31124	1454	1457	0.02824	(mV/V)/g
		y	right	ENDEVCO 7264-2000	J30554	1262	1272	0.03206	(mV/V)/g
		z	top	ENDEVCO 7264-2000	J31347	1283	1312	0.02609	(mV/V)/g
Pelvis	Triaxial Accel.	x	front	ENDEVCO 7264-2000	J31453	1455	1457	0.02552	(mV/V)/g
		y	left	ENDEVCO 7264-2000	J31448	1262	1272	0.02822	(mV/V)/g
		z	bottom	ENDEVCO 7264-2000	J31438	1340	1355	0.02541	(mV/V)/g
Left Femur	Upper LC	fx	topsurface - front	DENTON 4509	75	349	349	0.0001724	(mV/V)/N
		fy	topsurface - right	DENTON 4509	75	349	349	0.0001737	(mV/V)/N
		fz	tension	DENTON 4509	75	699	699	0.00009565	(mV/V)/N
		mx	topsurface - front	DENTON 4509	75	350	350	0.007402	(mV/V)/Nm
	Uniaxial Accel.	y1	left	ENDEVCO 7264-2000	J30549	1407	1413	0.02972	(mV/V)/g
		y2	right	ENDEVCO 7264-2000	J27777	1187	1188	0.02238	(mV/V)/g
Angular Accel. (broken)	x	back	ENDEVCO 7302B-50000					(mV/V)/(rad/s/s)	
Left Tibia	Uniaxial Accel.	y1	left	ENDEVCO 7264B-2000	B11864	610	642	0.02309	(mV/V)/g
		y2	right	ENDEVCO 7264-2000	J30443	1406	1412	0.02815	(mV/V)/g
	Angular Accel. (broken)	x	back	ENDEVCO 7302B-50000					(mV/V)/(rad/s/s)
	Upper LC	fx	topsurface - front	DENTON 4509	77	349	349	0.0001765	(mV/V)/N
		fy	topsurface - right	DENTON 4509	77	349	349	0.0001764	(mV/V)/N
		fz	tension	DENTON 4509	77	700	700	0.00009706	(mV/V)/N
		mx	topsurface - front	DENTON 4509	77	350	350	0.007515	(mV/V)/Nm
	Lower LC	fy	topsurface - right	DENTON 4354	80	349	350	0.0001742	(mV/V)/N
		fz	tension	DENTON 4354	80	698	698	0.00009841	(mV/V)/N
		mx	topsurface - front	DENTON 4354	80	350	350	0.007668	(mV/V)/Nm

* The excitation voltages of all sensors should be 10 V.

* Sensor polarity is + when the load to the sensor is along the direction.

* Two angular accelerometers on femur and tibia are broken now.

Two uniaxial accelerometers (y direction) have been attached on femur and tibia as the substitutes for angular accelerometers. The angular acceleration of femur or tibia should be calculated with two uniaxial accelerometers.

8.7. Channels from each test

Measurement	Designation
Sled Acceleration	SLDXG
Sled Velocity	SLDXV
Sled Velocity (Filtered)	SLDXVI
Sled Displacement (used for placing dummy)	SLDXDI
Head X Acceleration	HEDXG
Head Y Acceleration	HEDYG
Head Z Acceleration	HEDZG
Head Resultant Acceleration	HEDRG
Upper Neck Y Force	NEKYF
Upper Neck Z Force	NEKZF
Upper Neck X Moment	NEKXM
Front Neck Cable Z Force	NKFZF
Lower Neck Y Force	NKLYF
Lower Neck Z Force	NKLZF
Lower Neck X Moment	NKLXM
Rear Neck Cable Z Force	NKRZF
Chest X Acceleration	CSTXG
Chest Y Acceleration	CSTYG
Chest Z Acceleration	CSTZG
Chest Resultant Acceleration	CSTRG
Pelvis X Acceleration	PEVXG
Pelvis Y Acceleration	PEVYG
Pelvis Z Acceleration	PEVZG
Pelvis Resultant Acceleration	PEVRG
Left Femur X Force	LFMXF
Left Femur Y Force	LFMYF
Left Femur Z Force	LFMZF
Left Femur X Moment	LFMXM
Proximal Lateral Left Femur Y Acceleration	FSLYG
Distal Medial Left Femur Y Acceleration	FIMYG
Proximal Lateral Left Tibia Y Acceleration	TSLYG
Distal Medial Left Tibia Y Acceleration	TIMYG
Upper Left Tibia X Force	TBLXF
Upper Left Tibia Y Force	TBLYF
Upper Left Tibia Z Force	TBLZF
Upper Left Tibia X Moment	TBLXM
Lower Left Tibia (Ankle) Y Force	ANLYF
Lower Left Tibia (Ankle) Z Force	ANLZF
Lower Left Tibia (Ankle) X Moment	ANLXM
Equivalent Neck Moment about the Occipital Condyle	NEKOM
Femur Angular Acceleration	FEMUR ANG ACCEL
Tibia Angular Acceleration	TIBIA ANG ACCEL